

World Journal of *Radiology*

World J Radiol 2015 February 28; 7(2): 28-56



Editorial Board

2014-2017

The *World Journal of Radiology* Editorial Board consists of 365 members, representing a team of worldwide experts in radiology. They are from 36 countries, including Afghanistan (1), Argentina (2), Australia (5), Austria (7), Belgium (2), Brazil (8), Canada (6), Chile (1), China (43), Croatia (1), Denmark (4), Egypt (6), France (5), Germany (22), Greece (10), India (12), Iran (6), Ireland (2), Israel (3), Italy (47), Japan (13), Netherlands (1), New Zealand (1), Pakistan (1), Poland (2), Portugal (1), Serbia (1), Singapore (3), Slovakia (1), South Korea (18), Spain (4), Sweden (2), Switzerland (4), Thailand (1), Turkey (26), United Kingdom (11), and United States (82).

EDITORS-IN-CHIEF

Kai U Juergens, *Bremen*
Edwin JR van Beek, *Edinburgh*
Thomas J Vogl, *Frankfurt*

GUEST EDITORIAL BOARD MEMBERS

Wing P Chan, *Taipei*
Chung-Huei Hsu, *Taipei*
Chin-Chang Huang, *Taipei*
Tsong-Long Hwang, *Taoyuan*
Jung-Lung Hsu, *Taipei*
Chia-Hung Kao, *Taichung*
Yu-Ting Kuo, *Tainan*
Hon-Man Liu, *Taipei*
Hui-Lung Liang, *Kaohsiung*
Chun Chung Lui, *Kaohsiung*
Sen-Wen Teng, *Taipei*
Yung-Liang (William) Wan, *Taoyuan*

MEMBERS OF THE EDITORIAL BOARD



Afghanistan

Takao Hiraki, *Okayama*



Argentina

Patricia Carrascosa, *Vicente Lopez*
Maria C Ziadi, *Rosario*



Australia

Lourens Bester, *Sydney*
Gemma A Figtree, *Sydney*

Stuart M Grieve, *Sydney*
Wai-Kit Lee, *Fitzroy*
Prabhakar Ramachandran, *Melbourne*



Austria

Herwig R Cerwenka, *Graz*
Gudrun M Feuchtnner, *Innsbruck*
Benjamin Henninger, *Innsbruck*
Rupert Lanzenberger, *Vienna*
Shu-Ren Li, *Vienna*
Veronika Schopf, *Vienna*
Tobias De Zordo, *Innsbruck*



Belgium

Steve Majerus, *Liege*
Kathelijne Peremans, *Merelbeke*



Brazil

Clerio F Azevedo, *Rio de Janeiro*
Patrícia P Alfredo, *São Paulo*
Eduardo FC Fleury, *São Paulo*
Edward Araujo Júnior, *São Paulo*
Wellington P Martins, *Ribeirao Preto*
Ricardo A Mesquita, *Belo Horizonte*
Vera MC Salemi, *São Paulo*
Claudia Szobot, *Porto Alegre*
Lilian YI Yamaga, *São Paulo*



Canada

Marie Arsalidou, *Toronto*
Otman A Basir, *Waterloo*

Tarik Zine Belhocine, *Toronto*
James Chow, *Toronto*
Tae K Kim, *Toronto*
Anastasia Oikonomou, *Toronto*



China

Hong-Wei Chen, *Wuxi*
Feng Chen, *Hangzhou*
Jian-Ping Chu, *Guangzhou*
Guo-Guang Fan, *Shenyang*
Bu-Lang Gao, *Shijiazhuang*
Qi-Yong Gong, *Chengdu*
Ying Han, *Beijing*
Xian-Li Lv, *Beijing*
Yi-Zhuo Li, *Guangzhou*
Xiang-Xi Meng, *Harbin*
Yun Peng, *Beijing*
Jun Shen, *Guangzhou*
Ze-Zhou Song, *Hangzhou*
Wai Kwong Tang, *Hong Kong*
Gang-Hua Tang, *Guangzhou*
Jie Tian, *Beijing*
Lu-Hua Wang, *Beijing*
Xiao-bing Wang, *Xi'an*
Yi-Gen Wu, *Nanjing*
Kai Wu, *Guangzhou*
Hui-Xiong Xu, *Shanghai*
Zuo-Zhang Yang, *Kunming*
Xiao-Dan Ye, *Shanghai*
David T Yew, *Hong Kong*
Ting-He Yu, *Chongqing*
Zheng Yuan, *Shanghai*
Min-Ming Zhang, *Hangzhou*
Yudong Zhang, *Nanjing*
Dong Zhang, *Chongqing*
Wen-Bin Zeng, *Changsha*

Yue-Qi Zhu, *Shanghai*



Croatia

Goran Kusec, *Osijek*



Denmark

Poul E Andersen, *Odense*

Lars J Petersen, *Aalborg*

Thomas Z Ramsøy, *Frederiksberg*

Morten Ziebell, *Copenhagen*



Egypt

Mohamed F Bazeed, *Mansoura*

Mohamed Abou El-Ghar, *Mansoura*

Reem HA Mohamed, *Cairo*

Mohamed R Nouh, *Alexandria*

Ahmed AKA Razek, *Mansoura*

Ashraf A Zytoon, *Shebin El-Koom*



France

Sabine F Bensamoun, *Compiègne*

Romarc Loffroy, *Dijon*

Stephanie Nougaret, *Montpellier*

Hassane Oudadesse, *Rennes*

Vincent Vinh-Hung, *Fort-de-France*



Germany

Henryk Barthel, *Leipzig*

Peter Bannas, *Hamburg*

Martin Beeres, *Frankfurt*

Ilja F Ciernik, *Dessau*

A Dimitrakopoulou-Strauss, *Heidelberg*

Peter A Fasching, *Erlangen*

Andreas G Schreyer, *Regensburg*

Philipp Heusch, *Duesseldorf*

Sonja M Kirchhoff, *Munich*

Sebastian Ley, *Munich*

Adel Maataoui, *Frankfurt am Main*

Stephan M Meckel, *Freiburg*

Hans W Muller, *Duesseldorf*

Kay Raum, *Berlin*

Dirk Rades, *Luebeck*

Marc-Ulrich Regier, *Hamburg*

Alexey Surov, *Halle*

Martin Walter, *Magdeburg*

Axel Wetter, *Essen*

Christoph Zilkens, *Düsseldorf*



Greece

Panagiotis Antoniou, *Thessaloniki*

Nikos Efthimiou, *Athens*

Dimitris Karnabatidis, *Patras*

George Latsios, *Athens*

Stylianios Megremis, *Iraklion*

Alexander D Rapidis, *Athens*

Kiki Theodorou, *Larissa*

Ioannis A Tsalafoutas, *Athens*

Evanthia E Tripoliti, *Ioannina*

Athina C Tsili, *Ioannina*



India

Ritesh Agarwal, *Chandigarh*

Chandan J Das, *New Delhi*

Prathamesh V Joshi, *Mumbai*

Naveen Kalra, *Chandigarh*

Chandrasekharan Kesavadas, *Trivandrum*

Jyoti Kumar, *New Delhi*

Atin Kumar, *New Delhi*

Kaushala P Mishra, *Allahabad*

Daya N Sharma, *New Delhi*

Binit Sureka, *New Delhi*

Sanjay Sharma, *New Delhi*

Raja R Yadav, *Allahabad*



Iran

Majid Assadi, *Bushehr*

SeyedReza Najafizadeh, *Tehran*

Mohammad Ali Oghabian, *Tehran*

Amir Reza Radmard, *Tehran*

Ramin Sadeghi, *Mashhad*

Hadi Rokni Yazdi, *Tehran*



Ireland

Tadhg Gleeson, *Wexford*

Frederik JAI Vernimmen, *Cork*



Israel

Dafna Ben Bashat, *Tel Aviv*

Amit Gefen, *Tel Aviv*

Tamar Sella, *Jerusalem*



Italy

Adriano Alippi, *Rome*

Dante Amelio, *Trento*

Michele Anzidei, *Rome*

Filippo F Angileri, *Messinas*

Stefano Arcangeli, *Rome*

Roberto Azzoni, *San Donato milanese*

Tommaso V Bartolotta, *Palermo*

Tommaso Bartalena, *Imola*

Livia Bernardin, *San Bonifacio*

Federico Boschi, *Verona*

Sergio Casciaro, *Lecce*

Emanuele Casciani, *Rome*

Musa M Can, *Napoli*

Alberto Cuocolo, *Napoli*

Michele Ferrara, *Coppito*

Mauro Feola, *Fossano*

Giampiero Francica, *Castel Volturno*

Luigi De Gennaro, *Rome*

Giulio Giovannetti, *Pisa*

Francesca Iacobellis, *Napoli*

Formato Invernizzi, *Monza Brianza*

Francesco Lassandro, *Naples*

Lorenzo Livi, *Florence*

Pier P Mainenti, *Napoli*

Laura Marzetti, *Chieti*

Giuseppe Malinverni, *Crescentino*

Enrica Milanese, *Turin*

Giovanni Morana, *Treviso*

Lorenzo Monti, *Milan*

Silvia D Morbelli, *Genoa*

Barbara Palumbo, *Perugia*

Cecilia Parazzini, *Milan*

Stefano Pergolizzi, *Messina*

Antonio Pinto, *Naples*

Camillo Porcaro, *Rome*

Carlo C Quattrocchi, *Rome*

Alberto Rebonato, *Perugia*

Giuseppe Rizzo, *Rome*

Roberto De Rosa, *Naples*

Domenico Rubello, *Rovigo*

Andrea Salvati, *Bari*

Sergio Sartori, *Ferrara*

Luca M Sconfienza, *Milano*

Giovanni Storto, *Rionero*

Nicola Sverzellati, *Parma*

Alberto S Tagliafico, *Genova*

Nicola Troisi, *Florence*



Japan

Yasuhiko Hori, *Chiba*

Hidetoshi Ikeda, *Koriyama*

Masahito Kawabori, *Sapporo*

Tamotsu Kamishima, *Sapporo*

Hiro Kiyosue, *Yufu*

Yasunori Minami, *Osaka-sayama*

Yasuhiro Morimoto, *Kitakyushu*

Satoru Murata, *Tokyo*

Shigeki Nagamachi, *Miyazaki*

Hiroshi Onishi, *Yamanashi*

Morio Sato, *Wakayama Shi*

Yoshito Tsushima, *Maebashi*

Masahiro Yanagawa, *Suita*



Netherlands

Willem Jan van Rooij, *Tilburg*



New Zealand

W Howell Round, *Hamilton*



Pakistan

Wazir Muhammad, *Abbottabad*



Poland

Maciej S Baglaj, *Wroclaw*

Piotr Czauderna, *Gdansk*



Portugal

Joao Manuel RS Tavares, *Porto*



Serbia

Olivera Ciraj-Bjelac, *Belgrade*



Singapore

Gopinathan Anil, *Singapore*

Terence KB Teo, *Singapore*

Cher Heng Tan, *Singapore*



Slovakia

Stefan Sivak, *Martin*



South Korea

Ki Seok Choo, *Busan*

Seung Hong Choi, *Seoul*

Dae-Seob Choi, *Jinju*

Hong-Seok Jang, *Seoul*

Yong Jeong, *Daejeon*

Chan Kyo Kim, *Seoul*

Se Hyung Kim, *Seoul*

Joong-Seok Kim, *Seoul*

Sang Eun Kim, *Seongnam*

Sung Joon Kwon, *Seoul*

Jeong Min Lee, *Seoul*

In Sook Lee, *Busan*

Noh Park, *Goyang*

Chang Min Park, *Seoul*

Sung Bin Park, *Seoul*

Deuk Jae Sung, *Seoul*

Choongsoo Shin, *Seoul*

Kwon-Ha Yoon, *Iksan*



Spain

Miguel A De Gregorio, *Zaragoza*

Antonio Luna, *Jaén*

Enrique Marco de Lucas, *Santander*

Fernando Ruiz Santiago, *Granada*



Sweden

Dmitry Grishenkov, *Stockholm*

Tie-Qiang Li, *Stockholm*



Switzerland

Nicolau Beckmann, *Basel*

Christian Boy, *Bern*

Giorgio Treglia, *Bellinzona*

Stephan Ulmer, *Kiel*



Thailand

Sirianong Namwongprom, *Chiang Mai*



Turkey

Kubilay Aydin, *Istanbul*

Ramazan Akdemir, *Sakarya*

Serhat Avcu, *Ankara*

Ayşe Aralasmak, *Istanbul*

Oktay Algin, *Ankara*

Nevbahar Akcar, *Meselik*

Bilal Battal, *Ankara*

Zulkif Bozgeyik, *Elazig*

Nazan Ciledag, *Aakara*

Fuldem Y Donmez, *Ankara*

Gulgun Engin, *Istanbul*

Ahmet Y Goktay, *Izmir*

Oguzhan G Gumustas, *Bursa*

Kaan Gunduz, *Ankara*

Pelin Ozcan Kara, *Mersin*

Kivanc Kamburoglu, *Ankara*

Ozgur Kilickesmez, *Istanbul*

Furuzan Numan, *Istanbul*

Cem Onal, *Adana*

Ozgur Oztekin, *Izmir*

Seda Ozbek (Boruban), *Konya*

Selda Sarikaya, *Zonguldak*

Figen Taser, *Kutahya*

Baran Tokar, *Eskisehir*

Ender Uysal, *Istanbul*

Ensar Yekeler, *Istanbul*



United Kingdom

Indran Davagnanam, *London*

M DC Valdés Hernández, *Edinburgh*

Alan Jackson, *Manchester*

Suneil Jain, *Belfast*

Long R Jiao, *London*

Miltiadis Krokidis, *Cambridge*

Pradesh Kumar, *Liverpool*

Peter D Kuzmich, *Derby*

Georgios Plataniotis, *Brighton*

Vanessa Sluming, *Liverpool*



United States

Garima Agrawal, *Saint Louis*

James R Brasic, *Baltimore*

Rajendra D Badgaiyan, *Buffalo*

Ulas Bagci, *Bethesda*

Anat Biegon, *Stony Brook*

Ramon Casanova, *Winston Salem*

Wenli Cai, *Boston*

Zheng Chang, *Durham*

Corey J Chakarun, *Long Beach*

Kai Chen, *Los Angeles*

Hyun-Soon Chong, *Chicago*

Marco Cura, *Dallas*

Ravi R Desai, *Bensalem*

Delia DeBuc, *Miami*

Carlo N De Cecco, *Charleston*

Timm-Michael L Dickfeld, *Baltimore*

Subba R Digumarthy, *Boston*

Huy M Do, *Stanford*

Todd A Faasse, *Grand Rapids*

Salomao Faintuch, *Boston*

Girish M Fatterpekar, *New York*

Dhakshinamoorthy Ganesan, *Houston*

Robert J Griffin, *Little Rock*

Andrew J Gunn, *Boston*

Sandeep S Hedgire, *Boston*

Timothy J Hoffman, *Columbia*

Mai-Lan Ho, *San Francisco*

Juebin Huang, *Jackson*

Abid Irshad, *Charleston*

Matilde Inglese, *New York*

El-Sayed H Ibrahim, *Jacksonville*

Paul R Julsrud, *Rochester*

Pamela T Johnson, *Baltimore*

Ming-Hung Kao, *Tempe*

Sunil Krishnan, *Houston*

Richard A Komoroski, *Cincinnati*

Sandi A Kwee, *Honolulu*

King Kim, *Ft. Lauderdale*

Guozheng Liu, *Worcester*

Yiyan Liu, *Newark*

Venkatesh Mani, *New York*

Lian-Sheng Ma, *Pleasanton*

Rachna Madan, *Boston*

Zeyad A Metwalli, *Houston*

Yilong Ma, *Manhasset*

Hui Mao, *Atlanta*

Feroze B Mohamed, *Philadelphia*

Gul Moonis, *Boston*

John L Noshier, *New Brunswick*

Rahmi Oklu, *Boston*

Aytekun Oto, *Chicago*

Bishnuhari Paudyal, *Philadelphia*

Rajul Pandya, *Youngstown*

Chong-Xian Pan, *Sacramento*

Jay J Pillai, *Baltimore*

Neal Prakash, *Duarte*

Reza Rahbar, *Boston*

Ali S Raja, *Boston*

Gustavo J Rodriguez, *El Paso*

David J Sahn, *Portland*

Steven Schild, *Scottsdale*

Ali R Sepahdari, *Los Angeles*

Li Shen, *Indianapolis*

JP Sheehan, *Charlottesville*

Atul B Shinagare, *Boston*

Sarabjeet Singh, *Boston*

Charles J Smith, *Columbia*

Kenji Suzuki, *Chicago*

Monvadi Srichai-Parsia, *Washington*

Sree H Tirumani, *Boston*

Hebert A Vargas, *New York*

Sachit Verma, *Philadelphia*

Yoichi Watanabe, *Minneapolis*

Li Wang, *Chapel Hill*

Carol C Wu, *Boston*

Shoujun Xu, *Houston*

Min Yao, *Cleveland*

Xiaofeng Yang, *Atlanta*

Qingbao Yu, *Albuquerque*

Aifeng Zhang, *Chicago*

Chao Zhou, *Bethlehem*

Hongming Zhuang, *Philadelphia*

**REVIEW**

- 28 Imaging and interventions in hilar cholangiocarcinoma: A review
Madhusudhan KS, Gamanagatti S, Gupta AK

ORIGINAL ARTICLE**Basic Study**

- 45 Evaluation of changes of intracranial blood flow after carotid artery stenting using digital subtraction angiography flow assessment
Wada H, Saito M, Kamada K

Retrospective Study

- 52 Transcranial Doppler screening in sickle cell disease: The implications of using peak systolic criteria
Naffaa LN, Tandon YK, Irani N

ABOUT COVER

Editorial Board Member of *World Journal of Radiology*, Alexey Surov, MD, PhD, N/A, Department of Radiology, Martin-Luther-University Halle-Wittenberg, Halle D-06097, Germany

AIM AND SCOPE

World Journal of Radiology (*World J Radiol*, *WJR*, online ISSN 1949-8470, DOI: 10.4329) is a peer-reviewed open access academic journal that aims to guide clinical practice and improve diagnostic and therapeutic skills of clinicians.

WJR covers topics concerning diagnostic radiology, radiation oncology, radiologic physics, neuroradiology, nuclear radiology, pediatric radiology, vascular/interventional radiology, medical imaging achieved by various modalities and related methods analysis. The current columns of *WJR* include editorial, frontier, diagnostic advances, therapeutics advances, field of vision, mini-reviews, review, topic highlight, medical ethics, original articles, case report, clinical case conference (clinicopathological conference), and autobiography.

We encourage authors to submit their manuscripts to *WJR*. We will give priority to manuscripts that are supported by major national and international foundations and those that are of great basic and clinical significance.

INDEXING/ABSTRACTING

World Journal of Radiology is now indexed in PubMed Central, PubMed, Digital Object Identifier, and Directory of Open Access Journals.

FLYLEAF

I-III Editorial Board

EDITORS FOR THIS ISSUE

Responsible Assistant Editor: *Xiang Li*
Responsible Electronic Editor: *Huan-Liang Wu*
Proofing Editor-in-Chief: *Lian-Sheng Ma*

Responsible Science Editor: *Xue-Mei Gong*
Proofing Editorial Office Director: *Xin-Xia Song*

NAME OF JOURNAL
World Journal of Radiology

ISSN
ISSN 1949-8470 (online)

LAUNCH DATE
December 31, 2009

FREQUENCY
Monthly

EDITORS-IN-CHIEF
Kai U Juergens, MD, Associate Professor, MRT und PET/CT, Nuklearmedizin Bremen Mitte, ZEMODI - Zentrum für morphologische und molekulare Diagnostik, Bremen 28177, Germany

Edwin JR van Beek, MD, PhD, Professor, Clinical Research Imaging Centre and Department of Medical Radiology, University of Edinburgh, Edinburgh EH16 4TJ, United Kingdom

Thomas J Vogl, MD, Professor, Reader in Health Technology Assessment, Department of Diagnostic and Interventional Radiology, Johann Wolfgang

Goethe University of Frankfurt, Frankfurt 60590, Germany

EDITORIAL OFFICE
Jin-Lei Wang, Director
Xiu-Xia Song, Vice Director
World Journal of Radiology
Room 903, Building D, Ocean International Center, No. 62 Dongsihuan Zhonglu, Chaoyang District, Beijing 100025, China
Telephone: +86-10-59080039
Fax: +86-10-85381893
E-mail: editorialoffice@wjnet.com
Help Desk: <http://www.wjnet.com/esps/helpdesk.aspx>
<http://www.wjnet.com>

PUBLISHER
Baishideng Publishing Group Inc
8226 Regency Drive,
Pleasanton, CA 94588, USA
Telephone: +1-925-223-8242
Fax: +1-925-223-8243
E-mail: bpgoffice@wjnet.com
Help Desk: <http://www.wjnet.com/esps/helpdesk.aspx>
<http://www.wjnet.com>

PUBLICATION DATE
February 28, 2015

COPYRIGHT
© 2015 Baishideng Publishing Group Inc. Articles published by this Open-Access journal are distributed under the terms of the Creative Commons Attribution Non-commercial License, which permits use, distribution, and reproduction in any medium, provided the original work is properly cited, the use is non commercial and is otherwise in compliance with the license.

SPECIAL STATEMENT
All articles published in journals owned by the Baishideng Publishing Group (BPG) represent the views and opinions of their authors, and not the views, opinions or policies of the BPG, except where otherwise explicitly indicated.

INSTRUCTIONS TO AUTHORS
Full instructions are available online at http://www.wjnet.com/1949-8470/g_info_20100316162358.htm.

ONLINE SUBMISSION
<http://www.wjnet.com/esps/>

Imaging and interventions in hilar cholangiocarcinoma: A review

Kumble Seetharama Madhusudhan, Shivanand Gamanagatti, Arun Kumar Gupta

Kumble Seetharama Madhusudhan, Shivanand Gamanagatti, Arun Kumar Gupta, Department of Radiodiagnosis, All India Institute of Medical Sciences, New Delhi, Delhi 110029, India

Author contributions: All the authors equally contributed to this work.

Conflict-of-interest: The authors declare that they have no competing interests.

Open-Access: This article is an open-access article which was selected by an in-house editor and fully peer-reviewed by external reviewers. It is distributed in accordance with the Creative Commons Attribution Non Commercial (CC BY-NC 4.0) license, which permits others to distribute, remix, adapt, build upon this work non-commercially, and license their derivative works on different terms, provided the original work is properly cited and the use is non-commercial. See: <http://creativecommons.org/licenses/by-nc/4.0/>

Correspondence to: Shivanand Gamanagatti, Additional Professor, Department of Radiodiagnosis, All India Institute of Medical Sciences, Ansari Nagar East, Gautam Nagar, New Delhi, Delhi 110029, India. shiv223@rediffmail.com

Telephone: +91-11-26594567

Fax: +91-11-26588660

Received: October 8, 2014

Peer-review started: October 8, 2014

First decision: November 1, 2014

Revised: November 14, 2014

Accepted: December 16, 2014

Article in press: December 17, 2014

Published online: February 28, 2015

form of biliary drainage and/or portal vein embolization. In inoperable cases, palliative interventions include biliary drainage, biliary stenting and intra-biliary palliative treatment techniques. Complete knowledge of application of various imaging modalities available and about the possible radiological interventions is important for a radiologist to play a critical role in appropriate management of such patients. We review the various imaging techniques and appearances of hilar cholangiocarcinoma and the possible radiological interventions.

Key words: Cholangiocarcinoma; Biliary malignancy; Imaging; Biliary intervention; Computed tomography; Magnetic resonance imaging

© **The Author(s) 2015.** Published by Baishideng Publishing Group Inc. All rights reserved.

Core tip: Poor prognosis of hilar cholangiocarcinoma mandates early diagnosis. The article outlines the performance of various imaging modalities in making a diagnosis and allows the readers to decide the appropriately modality in a given case. Further, the brief descriptions of a wide range of radiological interventions in hilar cholangiocarcinoma educate the readers about the available options and choose them judiciously.

Abstract

Hilar cholangiocarcinoma is a common malignant tumor of the biliary tree. It has poor prognosis with very low 5-year survival rates. Various imaging modalities are available for detection and staging of the hilar cholangiocarcinoma. Although ultrasonography is the initial investigation of choice, imaging with contrast enhanced computed tomography scan or magnetic resonance imaging is needed prior to management. Surgery is curative wherever possible. Radiological interventions play a role in operable patients in the

Madhusudhan KS, Gamanagatti S, Gupta AK. Imaging and interventions in hilar cholangiocarcinoma: A review. *World J Radiol* 2015; 7(2): 28-44 Available from: URL: <http://www.wjgnet.com/1949-8470/full/v7/i2/28.htm> DOI: <http://dx.doi.org/10.4329/wjr.v7.i2.28>

INTRODUCTION

Cholangiocarcinoma (CC) is a malignant tumor of the biliary tree, originating from the bile duct epithelium. It is the second most common biliary

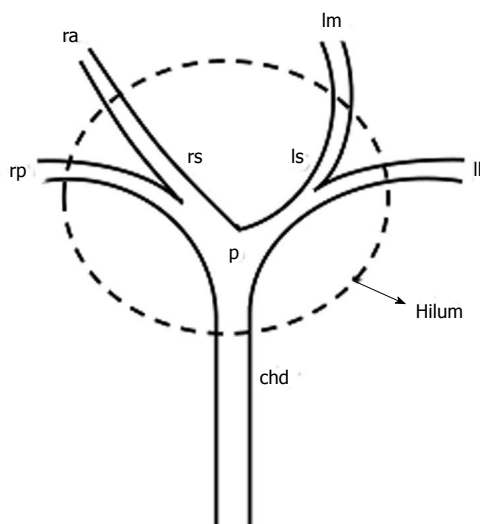


Figure 1 Schematic diagram showing structures forming hilum. chd: Common hepatic duct; ll: Left lateral segmental duct; lm: Left medial segmental duct; ls: Left secondary confluence; p: Primary biliary confluence; ra: Right anterior segmental duct; rp: Right posterior segmental duct; rs: Right secondary confluence.

tract malignancy, after carcinoma of gall bladder and second most common primary hepatic malignancy after hepatocellular carcinoma. The occurrence of the disease is increasing worldwide with an incidence of 1-2/100000^[1]. The symptoms at presentation are mostly non-specific and occur late in the course of the disease. Further, hilar masses invade adjacent vascular structures early and curative surgery is possible in less than half of the cases^[2]. The tumor has very poor prognosis with 5-year survival of about 5%^[3]. Hence, early diagnosis and curative surgery is needed to improve survival in these patients. We describe the various imaging modalities used in the diagnosis of CC and its appearances in these modalities. We further discuss various interventional radiological procedures playing role in management of patients with CC.

Cholangiocarcinoma can arise from any part of the biliary tree and depending on the location, they have been classified into three types - peripheral CC (or intrahepatic CC), hilar CC (or Klatskin tumor) and distal CC^[4]. Hilar CC is the most common variety forming about 40%-60% of all cases; distal CC forms 30%-42% and intrahepatic CC forms 5%-10%^[5,6]. Intrahepatic CC typically arise from beyond second order bile ducts whereas distal CC arise from extrahepatic common bile duct. Bismuth has classified hilar cholangiocarcinoma into four types depending on the location and extent of involvement bile ducts^[7]. Involvement of common hepatic duct (CHD) alone is defined as type 1, involvement of CHD and primary biliary confluence (PBC) as type 2, involvement of CHD, PBC and right or left hepatic ducts as type 3a or 3b respectively and involvement of CHD, PBC and both hepatic ducts or multifocal tumor as type 4.

Hilar cholangiocarcinoma (HiCC) is the most common anatomical type of CC. Although it can involve both intrahepatic and extrahepatic bile ducts, it is considered as a type of extrahepatic CC according to WHO classification^[8]. The tumor may arise from primary biliary confluence, right or left hepatic ducts, secondary biliary confluence or distal second order bile ducts (which together form the hilum) (Figure 1)^[9]. Although, the lesion is mostly extrahepatic, it may also extend intrahepatically and thus some use the term perihilar CC for the same. Macroscopically, HiCC has been classified into three types based on the growth pattern on gross specimen^[10]. They include nodular, periductal infiltrating and papillary types, of which the periductal infiltrating variety is the most common type (Figure 2). The nodular type begins as a small mucosal nodule and grows beyond the walls of the bile ducts to form a mass^[11]. The bile duct is obstructed at an early stage. Periductal-infiltrating type grows along the walls of the bile ducts causing its thickening and irregular luminal narrowing. Associated desmoplastic reaction may show smooth stenosis of the bile ducts adjacent to the tumor. Papillary tumor arises as a mucosal polypoidal or sessile lesion remains limited to the bile duct wall till late stages. This variety has better prognosis compared to the other two types. Histologically, about 90% of HiCC are adenocarcinomas, which range from well differentiated to poorly differentiated glands^[9]. Microscopically, the tumor consists of glands or tubules with fibrous stroma and inflammatory cells. Perineural, perilymphatic and perivenous invasion may be seen, of which the former is characteristic.

CLINICAL FEATURES

Due to the location of the tumor, even small masses produce biliary obstruction at an early stage and most patients present with obstructive jaundice. Other symptoms at presentation include anorexia, weight loss, right upper quadrant pain and pruritus. Patients may present with high-grade fever associated with chills and rigors due to cholangitis. Various risk factors predispose to the development of CC. These include primary sclerosing cholangitis, hepatolithiasis, liver fluke infection (*Opisthorchis viverrini* and *Clonorchis sinensis*), choledochal cyst and inflammatory bowel disease^[12]. Hepatitis B and C viruses have also been associated with increased risks of CC.

RADIOLOGICAL IMAGING

Imaging evaluation of HiCC is very important for accurate staging of the tumor and possible curative surgical resection. Assessment of longitudinal and extra-ductal extent of the tumor is critical as it defines treatment planning. However, varying

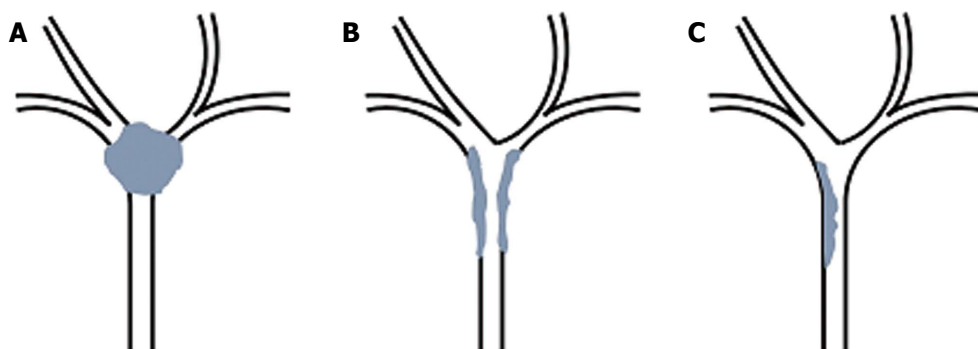


Figure 2 Schematic diagram showing three morphological types of hilar cholangiocarcinoma. A: Nodular variety; B: Periductal infiltrating; C: Intraductal papillary.

morphologies of HiCC may result in over or under-estimation of the tumor extent along the ducts and result in failure of curative treatment^[13]. Local extension of the tumor which suggest non-resectability on imaging include involvement of bilateral secondary biliary confluence, portal vein of one lobe and hepatic artery of other lobe, proper hepatic artery, main portal vein, hepatic artery or portal vein of one lobe with atrophy of other lobe. Ultrasonography, computed tomography (CT) and magnetic resonance imaging (MRI) are the most common non-invasive imaging modalities which are used in the diagnosis and staging of HiCC. Other less commonly used techniques are invasive and include percutaneous transhepatic cholangiography (PTC) and endoscopic retrograde cholangiography (ERC).

ULTRASONOGRAPHY

Sonography is the initial investigation which is performed in most patients presenting with obstructive jaundice or abdominal pain. In addition to detection of CC, it helps in excluding other causes of obstructive jaundice, primarily gall stones. The most common finding is dilatation of intrahepatic bile ducts^[14]. The union of right and left hepatic ducts is usually not visualized. At the site of obstruction, tumor may be seen with the currently available equipments. The primary tumor is most commonly isoechoic on ultrasonography (USG) (65%), but may be hypoechoic (21%) or hyperechoic (15%) (Figure 3)^[15]. Thenodular and papillary varieties can be seen as ill-defined lesions at the primary biliary confluence. The infiltrating variety may be seen as irregular isoechoic wall thickening of the right or left hepatic or proximal common hepatic ducts (Figure 3C). Lobar atrophy is a less common finding and is suggested by crowding of the dilated ducts and smaller size of the lobe (Figure 3D). This occurs when there is dominant involvement of one duct than the other. Lobar atrophy is seen in about 14% of patients with CC^[16]. Sonography also helps in evaluation of vascular structures, regional nodes and liver. The accuracy of lesion detection

on USG is about 82% and the sensitivity and specificity of portal vein involvement is 75%-83% and 93%-100%, respectively^[15,17]. USG has low accuracy for hepatic artery involvement. Contrast enhanced USG is an additional technique which can be performed in arterial, venous and delayed phases for better visualization and characterization of the tumor^[18,19]. Administration of USG contrast agents variably improves detection of primary lesion, the sensitivity of which may reach up to 100%^[20].

Endoscopic ultrasonography (EUS) is a technique where a high-frequency ultrasound probe is attached to the end of the endoscope. This helps in better visualization of hilar masses through stomach or duodenum^[21]. The benefits of EUS include no interference due to bowel gas (as seen with trans-abdominal USG), better visualization of mass and loco-regional lymph nodes and ability to obtain fine needle aspiration (FNA) or biopsy from the mass and nodes. The sensitivity and specificity of EUS in diagnosing and staging cholangiocarcinoma is 94% and 85% respectively^[22]. The diagnostic sensitivity and specificity of EUS with the use of FNAC for suspected HiCC is 89% and 100% respectively^[23]. Intraductal USG (IDUS) is another technique of using a high-resolution USG probe through either ERC or percutaneous transhepatic biliary drainage (PTBD) route^[24]. Hilar lesions are seen as hypoechoic masses around the biliary channels with irregular outline. This technique, when used with ERC has a sensitivity and specificity of 90% and 93%^[25]. However, visualization of deeper structures like vessels and nodes is difficult.

CT

CT scan is the most common widely used modality used for detection and staging of HiCC. Multidetector CT (MDCT) scan offers excellent spatial resolution and fast scanning and optimally depicts relation of the tumor with hepatic artery and portal vein^[26,27]. Multiplanar reformats (MPR) and maximum and minimum intensity projections are useful in accurately demonstrating ductal and vascular invasion (Figure 4).

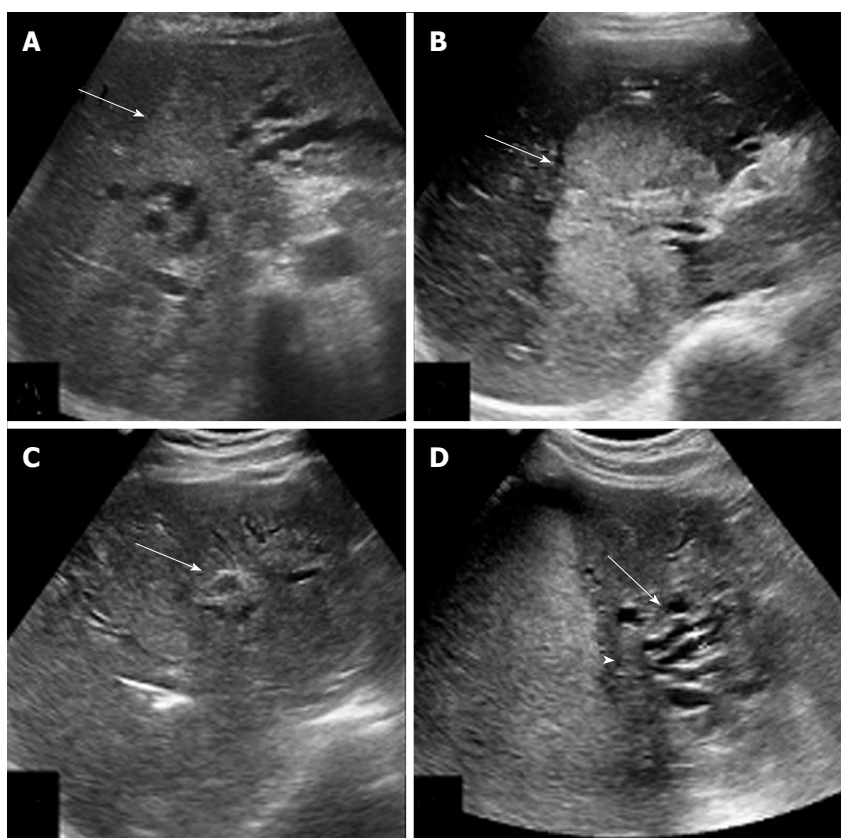


Figure 3 Ultrasonographic appearances of hilar cholangiocarcinoma. A: Isoechoic lesion (arrow) involving primary biliary confluence; B: Hyperechoic mass (arrow) involving hilum; C: Infiltrative lesion (arrow) with periductal wall thickening; D: Atrophy of left lobe with crowding of bile ducts (arrow) due to isoechoic hilar mass (arrow head).

MDCT has an accuracy of about 86% in assessment of ductal extent of HiCC^[28]. The sensitivity and specificity of MDCT in evaluation of portal vein, hepatic artery and lymph node involvement are 89% and 92%, 84% and 93%, and 61% and 88%, respectively.

The routine protocol for performing a CT scan in patients with suspected HiCC includes an arterial phase (25-35 s after beginning of contrast injection), portal venous phase (70-80 s) and delayed phase (180 s). Oral contrast is usually neutral or negative. Positive oral contrast is not given as it interferes with formation of MPRs. The arterial phase, demonstrates involvement of arteries (importantly main, right or left hepatic artery) by the tumor and also any variations in the arterial anatomy, which is useful for the surgeon. Portal venous phase reveals involvement of main portal vein or its first order branches. Further, this phase also better demonstrates primary tumor, liver metastases and extrahepatic spread (nodes, peritoneum) (Figure 5)^[29]. Delayed phase is useful in demonstration of primary mass which shows enhancement in delayed phase due to its scirrhous nature (Figure 6)^[30]. Oblique and curved MPRs show involvement of biliary tree and vessels better than the axial images and improve diagnostic accuracy^[29]. An additional and

important role of MDCT is in assessment of volume of future liver remnant (FLR) prior to surgery. The volume of FLR can be calculated either automatically or manually (Figure 7). Depending on the FLR volume in relation to body weight, either surgery can be planned directly or portal vein embolization may be performed to increase its volume. MDCT cholangiography without administration of biliary contrast agent can be done with volume rendering after adjusting the rendering parameters^[26]. This technique has a sensitivity and specificity of about 94% each in diagnosis of malignant biliary obstruction.

Nodular or mass-forming CC typically show thick irregular peripheral or heterogeneous enhancement in the arterial phase images with gradual centripetal enhancement in portal venous and delayed phase images (Figure 8)^[31]. However, very often the mass is small and may be difficult to visualize. Periductal infiltrating lesions typically show wall thickening and enhancement, which may completely obliterate the lumen. The lesion is usually hypoenhancing and may show enhancement in the delayed phase (Figure 9); occasionally it can enhance in arterial phase^[30]. Intraductal papillary lesions show single or multiple intraluminal polypoidal soft tissue which show contrast enhancement and distend the lumen of the

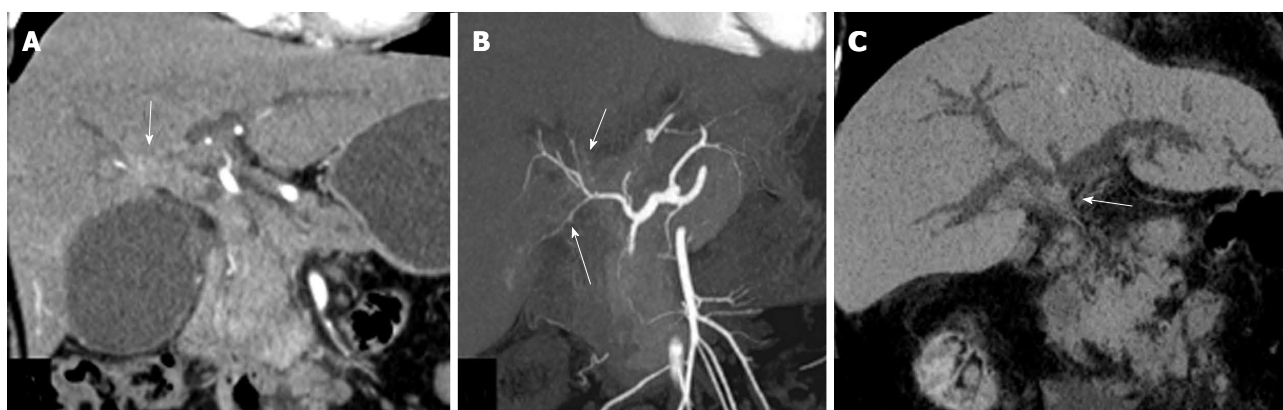


Figure 4 Post processing of computed tomography scan. A: Coronal reformat showing ill-defined enhancing mass (arrow) in relation to hilum and common hepatic duct; B: Coronal thick maximum intensity projection showing same mass as in A (short arrow) with irregularity of right posterior hepatic artery (long arrow); C: Minimum intensity projection showing the extent of biliary involvement by the mass (arrow).

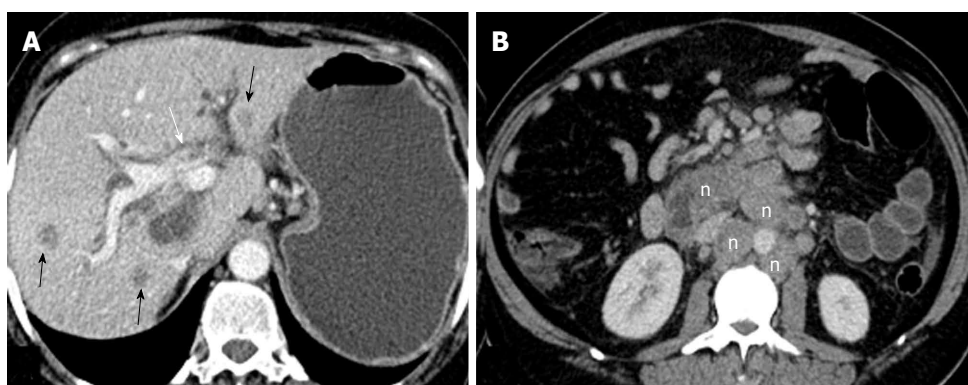


Figure 5 Axial contrast enhanced venous phase images. A: Showing hilar mass (white arrow) with multiple liver metastases (black arrows); B: Showing multiple metastatic retroperitoneal nodes (n).

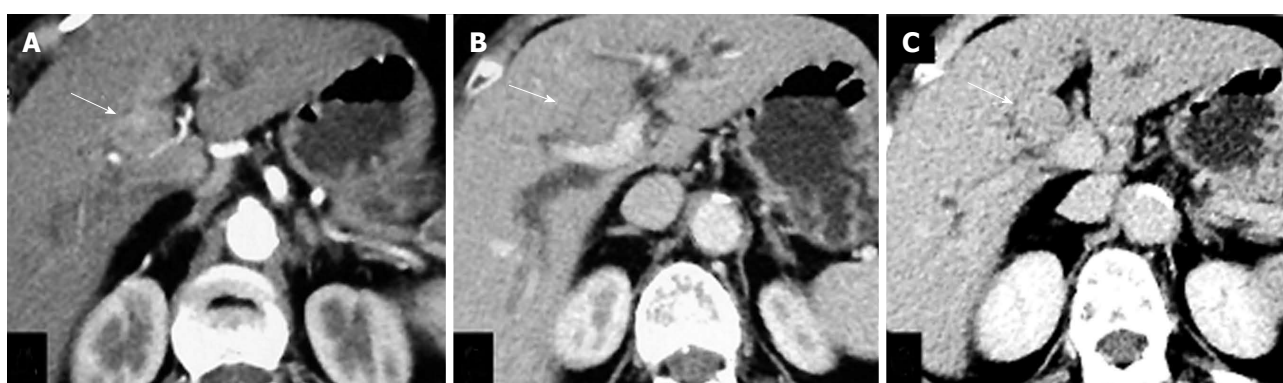


Figure 6 Axial contrast enhanced computed tomography scan in arterial (A), venous (B) and delayed (C) phases showing mild enhancement of the lesion (arrow) in arterial phase with persistence of enhancement in venous and delayed phases suggesting scirrhus nature of the lesion.

bile duct (Figure 10). Extension beyond the bile duct wall and lymph node involvement is uncommon. In addition to the primary lesion, CT scan also shows dilatation of the bile ducts upto the lesion and atrophy or hypertrophy of the lobes or segments (Figure 11). As with any other malignant tumors, vascular invasion is suggested by the presence of soft tissue encasing the vessel, large area of contact, narrowing of the calibre and complete luminal

obstruction (Figure 12).

MRI

Magnetic resonance cholangio-pancreatography (MRCP) is a heavily T2-weighted sequence used for demonstration of biliary channels and is as accurate as ERCP^[32]. Its advantages over ERCP include its non-invasiveness, its ability to visualize ducts

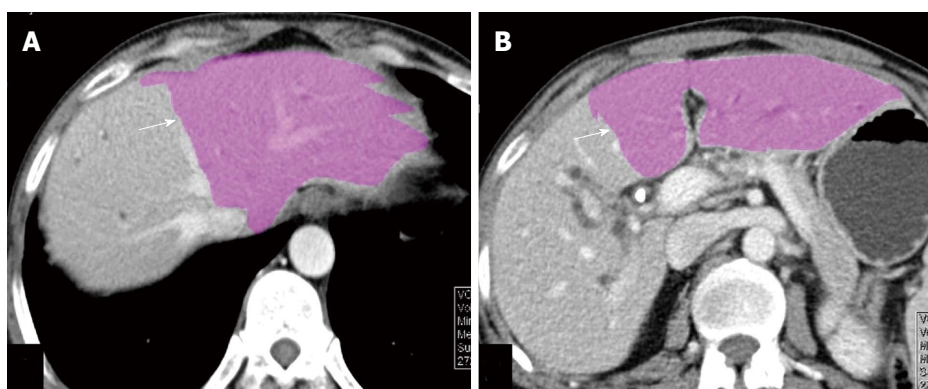


Figure 7 Axial venous phase computed tomography images (A and B) showing automated volumetry map with colour coding indicating the volume of future liver remnant (arrow).



Figure 8 Axial contrast enhanced computed tomography scan in arterial (A), venous (B) and delayed (C) phases of nodular variety of hilar cholangiocarcinoma (arrow) showing mildly enhancing ill-defined mass lesion in arterial phase with increasing enhancement in venous and delayed phases.



Figure 9 Axial (A) and coronal (B) images of venous phase of computed tomography scan of periductal infiltrating type of hilar cholangiocarcinoma showing wall thickening and enhancement of proximal common hepatic duct (arrow) causing luminal obstruction.

proximal to the obstruction and better visualization of the mass and non-requirement of contrast. Thin sections of MRCP and 3D-MRCP sequence further improve accuracy of lesion demonstration. MRI with gadolinium based contrast agents accurately depicts the mass, local extension, vascular involvement and regional metastases^[13,33]. The benefits of MRI over CT scan include no radiation, higher soft tissue contrast which helps in better demonstration of

tumor extent and better demonstration of biliary tree. MRI has its own share of limitations including longer acquisition times, motion artifacts, lower spatial resolution and lower accuracy in the presence of stents^[29]. The accuracy of MRI with MRCP in the prediction of involvement of biliary confluence, hepatic artery, portal vein and lymph node is 89%, 86%, 96% and 74%, respectively^[13].

Routine evaluation requires MRCP and MRI

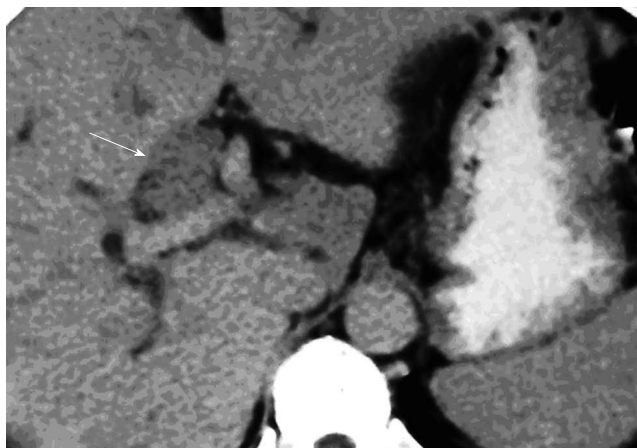


Figure 10 Axial contrast enhanced computed tomography scan in venous phase of papillary type of hilar cholangiocarcinoma showing minimally enhancing intraductal polypoidal lesion (arrow) causing distension of the duct.



Figure 11 Axial computed tomography images showing atrophy of right lobe (r) due to hilar mass (arrow) in A, and atrophy of left lobe (l) caused by a mass (arrow) in B.

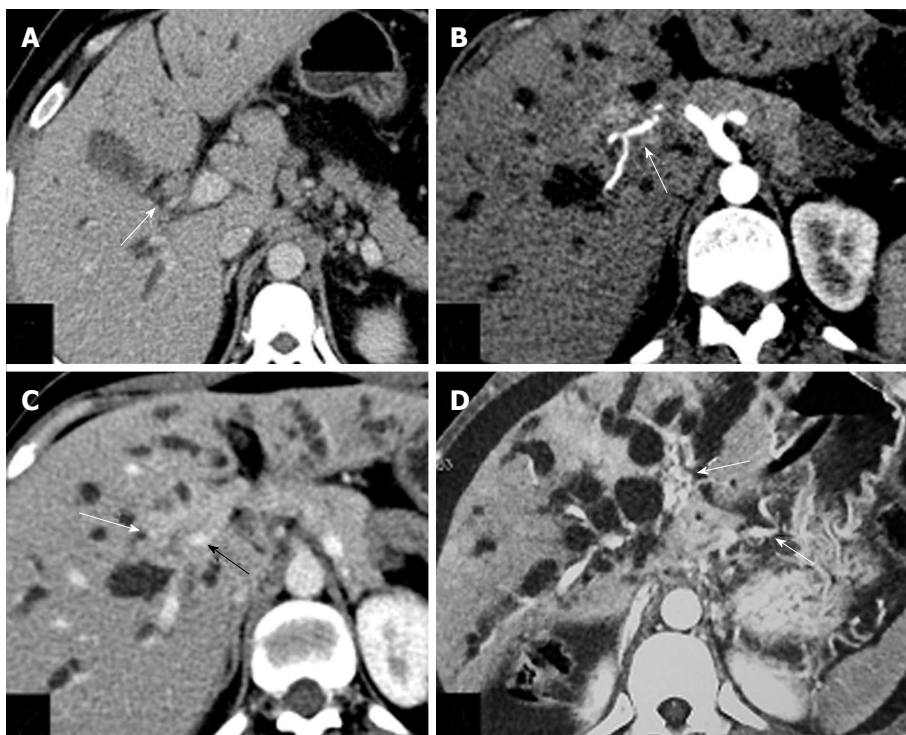


Figure 12 Axial computed tomography scan images showing vascular invasion. A: Small hilar mass (white arrow) abutting right hepatic artery posteriorly; B: Hilar mass (white arrow) encasing right hepatic artery causing irregularity in outline; C: Ill-defined hilar mass (white arrow) encasing portal vein and causing its narrowing (black arrow); D: Multiple collaterals (white arrows) seen in periportal and perigastric location due to portal vein obstruction.

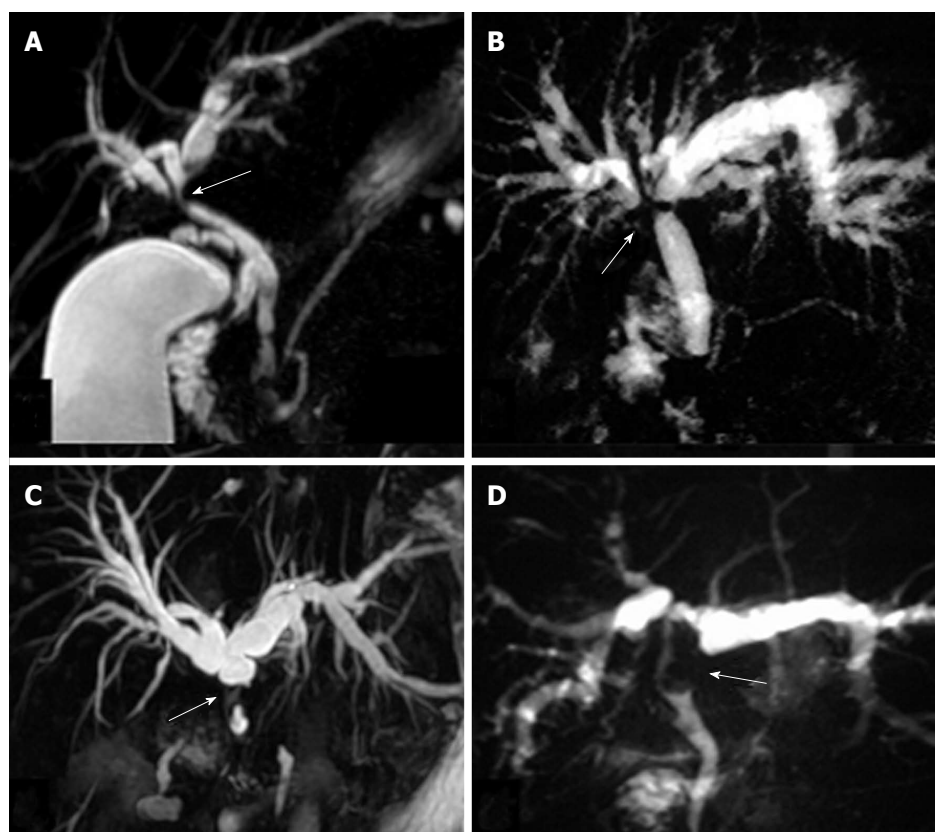


Figure 13 Magnetic resonance cholangio-pancreatography images showing various appearances of hilar cholangiocarcinoma. A: Smooth luminal narrowing (arrow); B: Complete hilar obstruction (arrow); C: Irregular asymmetric complete obstruction (arrow); D: Intraluminal filling defect (arrow).



Figure 14 Case of nodular type of hilar cholangiocarcinoma. A: Axial T2-weighted magnetic resonance image show hypointense hilar mass (arrow) with biliary dilatation; B and C: Axial T1-weighted magnetic resonance images in arterial (B) and venous (C) phases showing mildly enhancing ill-defined mass lesion (arrow) encasing right hepatic artery and left portal vein.

with contrast in multiple phases, similar to that of multiphase CT scan. On MRCP, the lesions cause irregular narrowing of the bile ducts, with or without obstruction, asymmetric luminal narrowing, abrupt luminal narrowing and as intraluminal filling defects (Figure 13). The appearance of the three morphological types of HiCC on contrast enhanced MRI is similar to that seen on CT scan (Figures 14 and 15). As in CT scan, the lesion shows peripheral or heterogeneous arterial enhancement with gradually increasing enhancement in the venous and delayed phases. Enhancement of ductal wall and

periductal infiltration is often better seen on MRI than on CT scan due to inherent higher contrast resolution of MRI. Diffusionweighted imaging (DWI) is useful in detecting smaller lesions (Figure 16). The b-values routinely used are 0, 500 and 800 s/mm². The technique has higher sensitivity and accuracy than MRI in detection of lesions and has high positive predictive value^[34]. Some inflammatory and benign lesions may mimic HiCC on MRI, but short segment involvement, irregular margins, asymmetric narrowing and diffusion restriction on DWI may point towards HiCC^[35]. The presence of stent affects

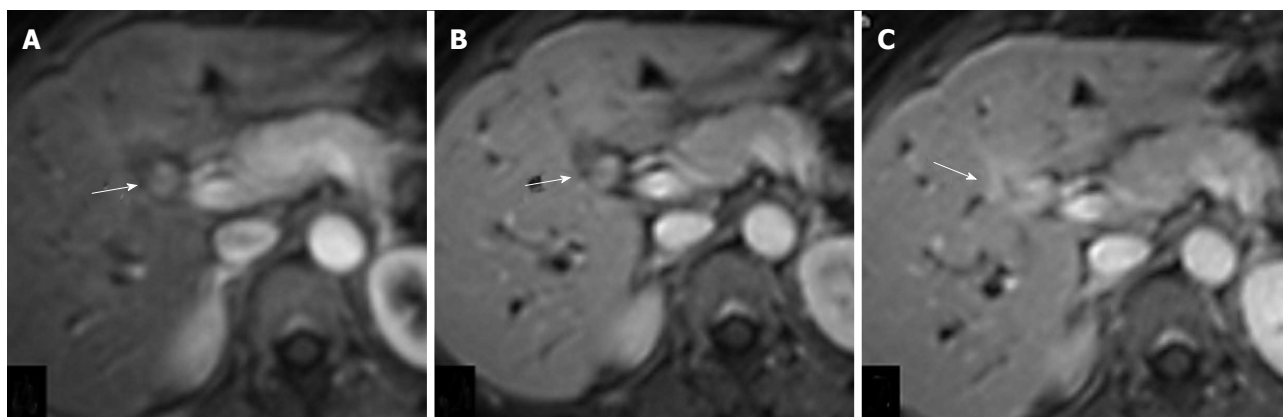


Figure 15 Axial contrast enhanced T1-weighted magnetic resonance images in arterial (A), venous (B) and delayed (C) phases of periductal infiltrating variety of hilar cholangiocarcinoma showing mildly enhancing thick walled proximal hepatic duct in arterial phase (arrow) with increasing contrast enhancement in venous and delayed phases.

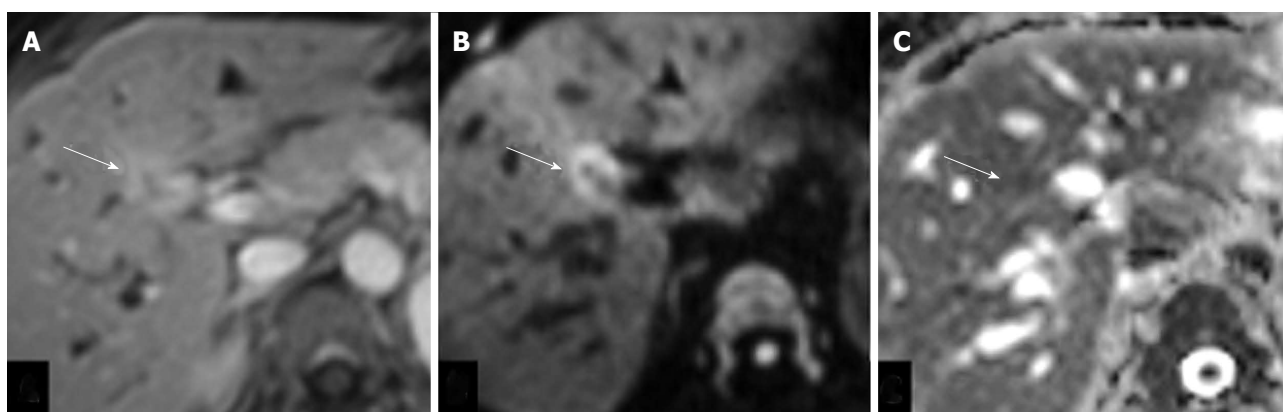


Figure 16 A case of periductal type of hilar cholangiocarcinoma. A: Axial T1-weighted contrast enhanced magnetic resonance (MR) image in delayed phase showing enhancing periductal lesion (arrow); B and C: Axial diffusion weighted b=800 MR images (B) and ADC map (C) showing diffusion restriction of the lesion.

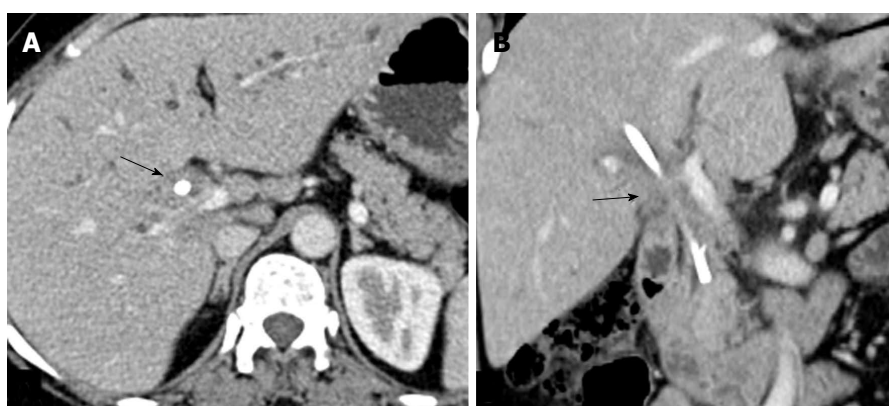


Figure 17 Axial (A) and coronal (B) computed tomography scan of a case of hilar cholangiocarcinoma after endoscopic stenting showing circumferential wall thickening of common hepatic duct around the stent. It would be difficult to differentiate this from reactive thickening.

evaluation of the tumor due to difficulty in assessing the level of obstruction as the bile ducts are decompressed after stenting and due to secondary sub-clinical cholangitis which cause wall thickening (Figure 17). Thus, imaging should be done prior to biliary decompression for accurate evaluation of the tumor.

POSITRON EMISSION TOMOGRAPHY CT

Cholangiocarcinomas express glucose transporter in higher concentration and take up ^{18}F Fluoro-deoxy Glucose (FDG). The sensitivity of detection depends on the morphological type and location of the tumor with lower rates of sensitivity seen in infiltrating

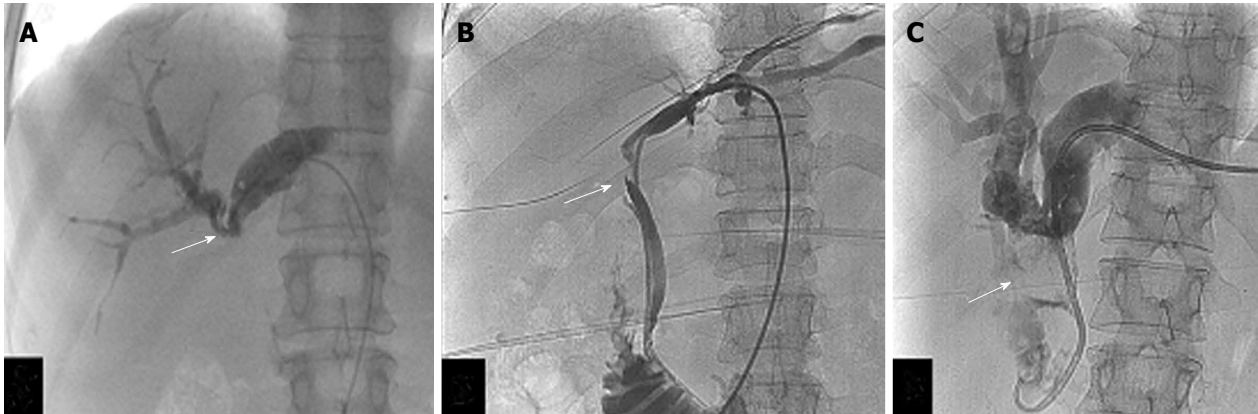


Figure 18 Percutaneous cholangiograms showing complete obstruction of common hepatic duct with patent primary biliary confluence (arrow, A), blocked primary biliary confluence with irregular outline (arrow, B) and intraluminal polypoidal filling defect (arrow, C).

Table 1 Bismuth-Corlette classification of hilar cholangiocarcinoma

Stage	Description
I	Tumor involving common hepatic duct without involvement of primary biliary confluence (confluence of right and left hepatic ducts) (Figure 19)
II	Tumor involving primary biliary confluence (Figure 20)
IIIa	Tumor involving primary biliary confluence and right secondary biliary confluence (confluence of right anterior and posterior sectoral ducts) (Figure 21)
IIIb	Tumor involving primary biliary confluence and left secondary biliary confluence (confluence of left medial and lateral sectoral ducts) (Figure 22)
IV	Tumor involving primary and both secondary biliary confluence (Figure 23)

types and extrahepatic cholangiocarcinoma^[36]. Nodular lesions show better uptake but infiltrating lesions are seen as streak-like uptake, which is sometimes difficult to detect. In the detection of primary tumor, FDG positron emission tomography CT (PET-CT) has a sensitivity, specificity and accuracy of 84%, 79% and 83%, respectively^[37]. However, for HiCC, sensitivity of PET-CT is lower than CT scan^[38]. Hence, routine use of PET-CT does not offer advantage over CT scan or MRI in the detection of HiCC. However, it has higher accuracy in the detection of metastatic regional lymph nodes and distant sites than other imaging modalities.

DIRECT CHOLANGIOGRAPHY

PTC and ERC are invasive techniques which involve injection of contrast directly into the bile ducts^[29]. In PTC, the dilated bile ducts are directly punctured under fluoroscopic or USG guidance through transhepatic route and contrast is injected antegradely to define the level and type of obstruction (Figure 18). In ERC, the duodenal ampulla is cannulated endoscopically and contrast is injected retrogradely to fill the bile ducts distal to the obstruction; proximal ducts may be visualized if obstruction is partial. Presence of short segment involvement, irregular stricture, asymmetric narrowing and nodularity suggests malignancy. Nodular type is usually seen as complete obstruction at primary biliary confluence^[39]. Short segment irregular or smooth narrowing is seen in case of periductal infiltrating variety and polypoidal or plaque

like filling defect in case of papillary type of HiCC. Additional benefits of PTC and ERCP include drainage of the obstructed system and ability to obtain brush cytology/biopsy.

Cholangioscopy is a technique of direct visualization of the tumor either through ERC route or PTBD route. It can help in differentiation of benign and malignant biliary strictures on the basis of presence of nodularity and irregularity of the mucosa and mucosal vessels^[40]. It has good accuracy in detection and evaluation of extent of HiCC which can be improved with the use of biopsy.

CLASSIFICATION AND STAGING

Bismuth-Corlette classified cholangiocarcinoma based on the longitudinal extent of the tumor^[41]. MRCP has high accuracy in classification of HiCC with an accuracy of 95% when compared to findings at surgery^[42]. The classification has been described in Table 1. This classification alone is not sufficient for assessing resectability of the tumor as it does not define lateral extension and it has little prognostic value^[43].

American Joint Committee on Cancer uses TNM classification for staging HiCC which is useful for selecting surgical candidates^[44]. "T" stands for primary tumor stage, "N" for nodal disease and "M" for metastases. The classification is as follows: (1) T stage: T1 - Tumor confined to bile duct, T2 - Tumor extending beyond the bile duct, this is further divided into T2a where there is involvement of



Figure 19 Schematic diagram and magnetic resonance cholangio-pancreatography image of type 1 hilar cholangiocarcinoma.

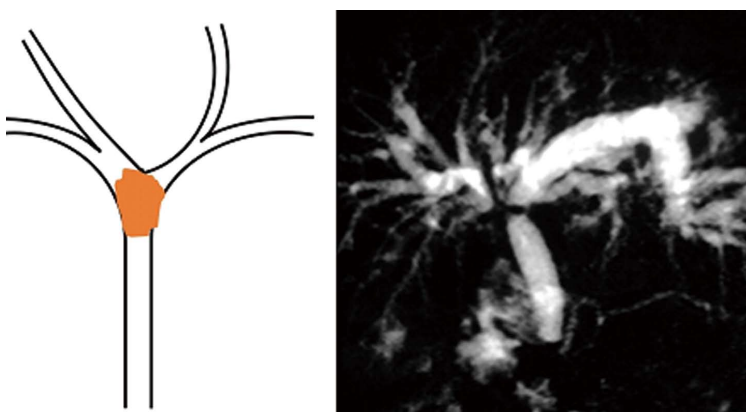


Figure 20 Schematic diagram and magnetic resonance cholangio-pancreatography image of type 2 hilar cholangiocarcinoma.

periductal fat and T2b where there is involvement of adjacent liver, T3 - Tumor involving unilateral portal vein or hepatic artery branches, T4 - Tumor involving one lobar portal vein branch and other lobar hepatic artery branch, main portal vein or common hepatic artery, second order bile ducts; (2) N stage: N0 - No lymph node involvement, N1 - Regional lymph nodes involvement (periductal or periportal nodes), N2 - Retroperitoneal nodes involvement; (3) M stage: M0 - No distant metastasis, M1 - Distant metastasis; and (4) Stages: I - T1 N0 M0, II - T2a-b N0 M0, III A - T3 N0 M0, III B - T1-3 N1 M0, IVA - T4 N0-1 M0, IVB - Any T N2 M0 or Any T Any N M1.

Imaging with multiphase CT scan and/or contrast enhanced MRI is helpful in accurately staging HiCC^[28]. Staging laparoscopy may rarely be needed when imaging findings are inconclusive.

RADIOLOGICAL INTERVENTIONS

Various radiological interventions are available in the management of HiCC, which could be either pre-operative (prior to definitive surgery) or palliative (in inoperable cases). Often the tumors are unresectable at the time of presentation and palliation is the only treatment possible to improve patients' quality of life^[2]. The main aim of palliation is to create a communication between the biliary system and small intestine to allow physiological drainage. This procedure reduces pain and relieves biliary obstruction and thus significantly decreases the

incidence of cholangitis and prepares the patient to receive chemotherapy. If it is done as a pre-operative procedure, it improves the liver function so that the patient can be treated surgically^[45].

Several safe and effective percutaneous radiological interventions are available in the management of HiCC. Although endoscopic drainage has the advantages of causing less pain, absence of an uncomfortable external drainage tube and less risk of biliary peritonitis, its success rate in too high obstructions is less and hence percutaneous technique is preferred^[46]. Cholangitis is seen in significantly higher number of patients as compared to percutaneous intervention as some of the obstructed ducts may not be drained^[45]. Various radiological interventional procedures include PTBD, biliary stenting (BS), intrabiliary tumor therapy and portal vein embolization (PVE). After the initial imaging, optimal further management is planned at the gastrointestinal-radiology meeting involving surgeons, gastroenterologists and radiologists.

PTBD

PTBD is the most common and well established interventional procedure performed in the management of HiCC. This is done either as a pre-operative procedure to improve liver functions or as a palliative procedure. Drainage of a single lobe (or at least 20% of liver parenchyma) is sufficient to relieve jaundice and improve liver functions^[47]. The



Figure 21 Schematic diagram and magnetic resonance cholangiopancreatography image of type 3A hilar cholangiocarcinoma.

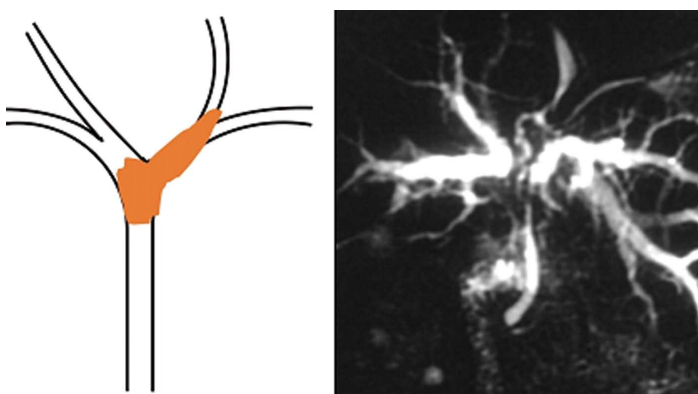


Figure 22 Schematic diagram and magnetic resonance cholangiopancreatography image of type 3B hilar cholangiocarcinoma.

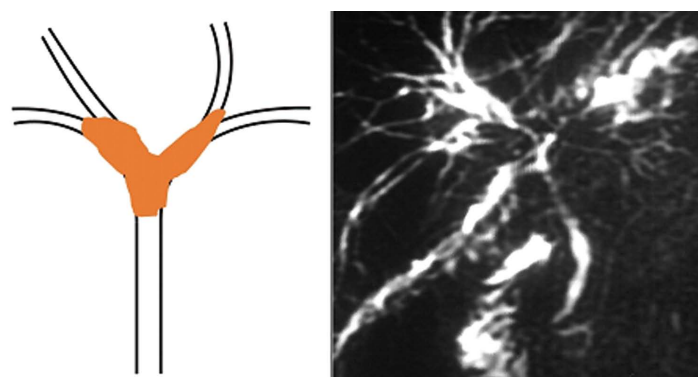


Figure 23 Schematic diagram and magnetic resonance cholangiopancreatography image of type 4 hilar cholangiocarcinoma.

primary biliary confluence is most often blocked in patients with HiCC and draining either the right or left lobe is adequate. The factors determining the selection of lobe to be drained are the size of the lobe and involvement of secondary biliary confluence. Prior imaging plays a crucial role in assessing the extent and severity of biliary dilatation and location of stricture. The larger lobe and one with patent secondary biliary confluence is preferred to allow maximum drainage. However, any dilated system could be a source of infection due to stasis and an attempt must be made to drain it, especially if it is infected. When unilateral drainage, which has lower incidence of complications, is planned, cholangiogram must be carefully done to avoid filling of the non-drainable biliary system and thus subsequent infection^[48]. If the primary biliary confluence is patent, either left or right

sided drainage can be done depending on the local practice, patient comfort and radiologist's expertise. Bilobar or multiple system drainage may also be done. In cases where there is atrophy of a lobe due to chronic biliary obstruction, the system may not need drainage as improvement in liver function is unlikely^[49]. But it needs drainage if this lobe is the source of cholangitis. No absolute contraindication exists for PTBD. Relative contraindications include bleeding diathesis, contrast allergies and ascites.

Prior to the procedure, patient preparation is needed. This includes correction of coagulation profile, if deranged and administration of a dose of broad spectrum antibiotic. Ascites should be drained before PTBD. The segmental duct (preferably segment 3 for left sided and segment 6 for right sided drainage) is punctured, using ultrasonography as guidance. The puncture needle is exchanged for

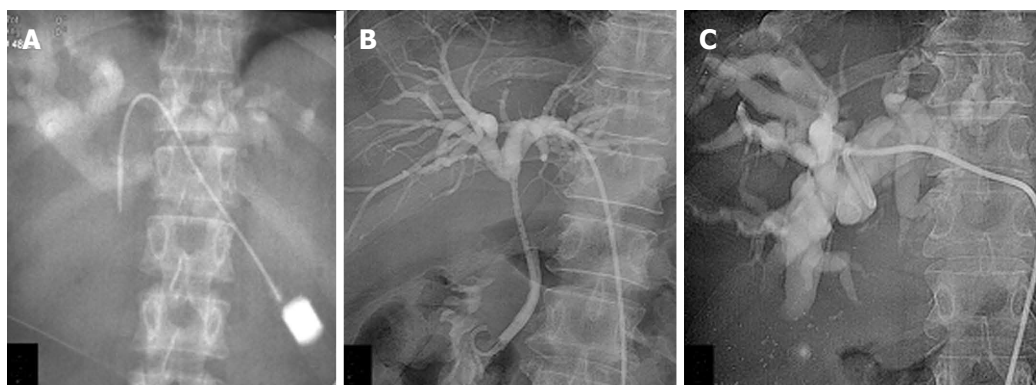


Figure 24 Types of biliary drainages. A: Initial cholangiogram showing dilated intrahepatic bile ducts with hilar obstruction; B: Cholangiogram after placement of ring biliary catheter (Internal-External drainage) showing opacification of bile ducts and duodenum; C: Cholangiogram after placement of external drainage pig-tail catheter.

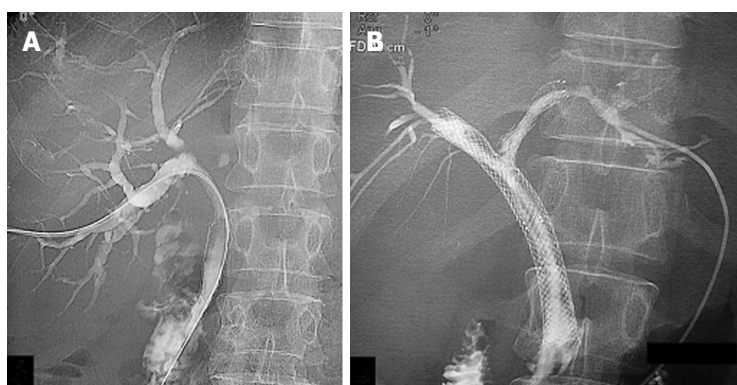


Figure 25 Types of biliary stenting. A: Cholangiogram after placement of unilobar (right sided) biliary metallic stent; B: Cholangiogram after bilobar stent placement showing free flow of contrast into duodenum across the stricture.

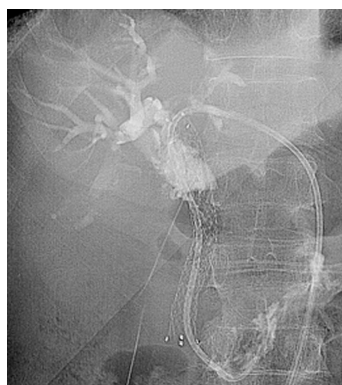


Figure 26 Percutaneous biliary drainage through ring biliary catheter after obstruction of biliary metallic stent due to tumor ingrowth.

a dilator over a guidewire, and check cholangiogram is performed to define the biliary anatomy (Figure 24A). Subsequently a guidewire is manipulated across the stricture following which the tract is dilated and an 8.3 F internal-external drainage catheter (Ring biliary catheter, Cook, Bloomington, IN) is placed across the stricture (Figure 24B). In cases where there is difficulty in crossing the stricture, an external drainage catheter is placed *in situ* (Figure 24C) and internal drainage is attempted two-four days later. This approach often helps in reducing the inflammation and edema and increases the chances of negotiating the stricture. Küçükay *et*

al^[50], in their study ($n = 256$) on percutaneous treatment of malignant biliary obstructions found that suprahilar lesions and lesions with flat or ovoid shape had higher failure rates. They suggested that an external drainage should be done after five unsuccessful attempts of internal drainage. Mueller *et al*^[51], reported easier catheterization of a stricture in a delayed second session due to straightened course of the guide wire directing into the lumen by decreased duct calibre above the obstruction, resolution of reactive edema at the site of obstruction and development of a tract around the catheter enabling the use of large-caliber catheters. An additional advantage of PTBD is the ability to obtain endobiliary tissue sample for histopathology using brush (for cytology) or forceps (for biopsy)^[52].

BILIARY STENTING

Biliary stenting is done in inoperable cases as a palliative measure. It can be done as a primary procedure or after PTBD. In primary stenting, once the stricture is crossed with guide-wire, stent can be deployed over the guide-wire across the obstruction. This reduces the incidence of procedure related complications compared to stenting done after PTBD^[53]. Self-expandablemetallic stents are preferred. Metallic stents have higher patency rates, lower overall cost and shorter hospital stay

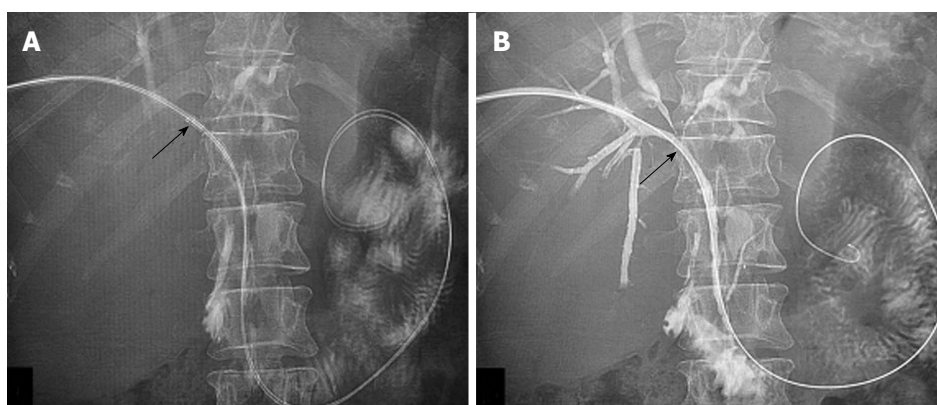


Figure 27 Percutaneous radiofrequency ablation for hilar cholangiocarcinoma. A: Pre-radiofrequency ablation (RFA) image with probe *in situ* (arrow); B: Cholangiogram after RFA showing opening of obstruction (arrow).

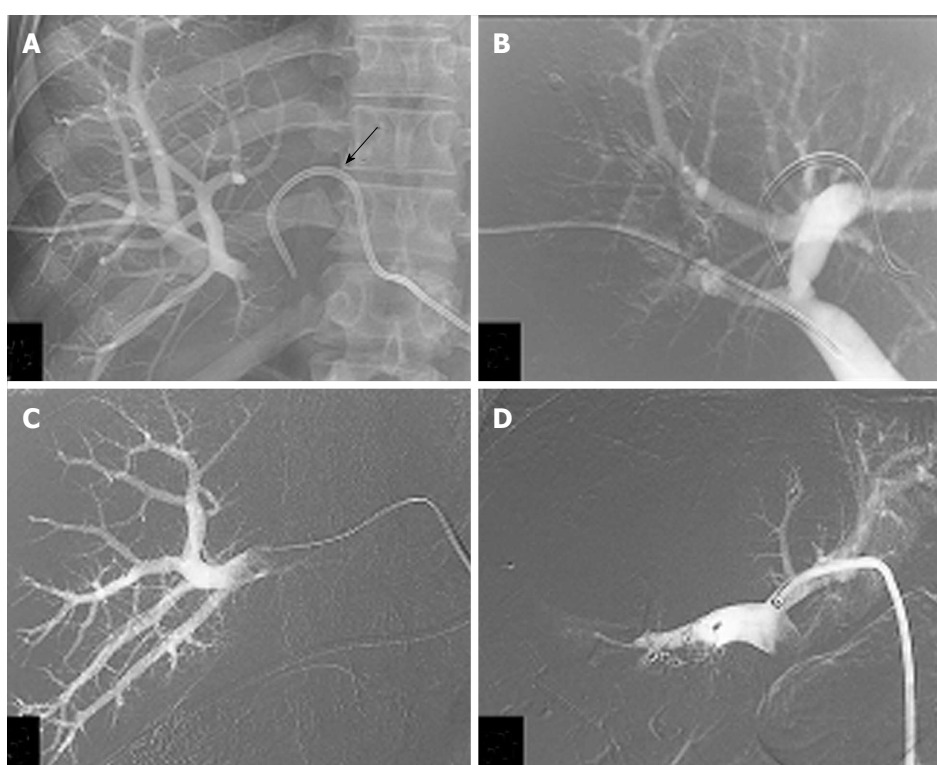


Figure 28 Right portal vein embolization with ipsilateral (A and B) and contralateral (C and D) approaches. A: Right portal venogram with ipsilateral approach. percutaneous transhepatic biliary drainage catheter is seen (arrow); B: Portal venogram after embolization of right portal vein with PVA and glue; C: Right portal venogram with contralateral approach; D: Portal venogram after embolization of right portal vein with glue and vascular plug.

than plastic stents (Figure 25)^[54]. Pre-stent balloon dilatation is usually avoided as it increases the risk of bleeding^[53]. The stent usually expands completely within 24-48 h and allows decompression of the biliary tree. If it does not adequately expand after 48 h, balloon dilatation of the stent may be done subsequently for adequate drainage. For masses involving the primary biliary confluence, two metallic stents (right and left side) can be placed in "Y" shape to drain both the systems (Figure 25B).

The biliary stent may get blocked by internal biliary sludge or by the tumor. Tumor ingrowth occurs when the tumor grows into the stent lumen through

the gaps between the struts of the stent. This may be dealt with endoscopically or percutaneously. Endoscopic placement of plastic stent through the blocked primary stent is often successful^[55]. Otherwise, percutaneous intervention in the form of balloon dilatation or placement of a smaller calibre coaxial stent or ring biliary catheter is done (Figure 26)^[55]. Use of covered metallic stents prevents tumor ingrowth and thus improves stent patency rates and reduces the incidence of re-intervention^[56]. Progression of the tumor may result in involvement of more proximal ducts and the stent may become ineffective. Such cases may need further drainage

which is often is difficult to achieve. Stent migration, a very rare complication, may require repeat procedure.

INTRA-BILIARY PALLIATIVE THERAPY

Intra-biliary brachytherapy or photodynamic therapy prior to stenting improves the life expectancy of patients with HiCC and also stent patency^[57]. The primary advantage of intraluminal brachytherapy over external beam radiotherapy is that higher doses of irradiation can be given without damaging adjacent normal tissues^[58]. This procedure is usually done through PTBD route, preferably after metallic stent placement. The iridium-192 strands are intraluminally placed at the site of the tumor or stricture through PTBD catheter. Chen *et al.*^[59], found 98% success rate of intraluminal brachytherapy using Iridium-192 in 34 patients of malignant biliary obstruction and concluded that intraluminal brachytherapy is a safe palliative therapy and improves patient survival. In photodynamic therapy, a photosensitizer is injected intravenously followed by application of light to the tumor, endoscopically or through PTBD route. The photosensitizer interacts with the light releasing free radicals and causing cell death. Lee *et al.*^[60] in their study ($n = 33$) found that photodynamic treatment prior to metallic stenting resulted in significantly longer stent patency and longer survival, with low risk of complications (17%).

RADIOFREQUENCY ABLATION

Radiofrequency ablation (RFA), a technique which causes coagulation necrosis of tissue, is well known in the treatment of hepatic tumors. Its use as a palliative procedure in unresectable HiCC has produced promising results^[61]. The procedure can be done either through transhepatic route with routine probes used for liver tumors or through endoscopic or PTBD route with the use of special endobiliary probe (Figure 27)^[62,63]. RFA in unresectable cases is a safe procedure and it improves stent patency and survival.

PVE

This procedure is done to induce hypertrophy of non-involved lobe of liver by HiCC if the remnant liver volume is insufficient to maintain normal body function. Although it is not specific for HiCC, it is done in a few such patients so that a curative surgery can be performed. Embolization of the portal vein branch of the lobe which is involved by the lesion and which would be subsequently resected is done to induce hypertrophy of the other lobe^[64,65]. Hypertrophy normally occurs in 2-4 wk after which surgery can be done. Various embolizing materials

are used including polyvinyl alcohol particles, gelatin sponge (gelfoam) and n-butyl cyanoacrylate (glue)^[66]. Vascular plugs can also be used in addition to these materials to increase the chance of hypertrophy.

The procedure can be performed puncturing either ipsilateral or contralateral portal vein branch under USG guidance. Once within the system, the puncture needle is exchanged for a catheter over a guide-wire. With the tip of the catheter sufficiently distal to the bifurcation, the embolizing material is injected till the flow slows down significantly (Figure 28). After embolization, the needle tract either can be left alone or can be embolized with a coil or gelatin sponge. Imaging is then usually performed after 3-4 wk and the volume of future liver remnant is measured. If it is adequate, curative surgery can be performed. The procedure has a technical success rate of 99.3%, clinical success rate of 96.1% and mean liver hypertrophy rate of 38%^[66].

CONCLUSION

HiCC is a common malignancy of the biliary tract and imaging with various modalities play an important role planning appropriate management. Selection of appropriate imaging modality is important to obtain complete information needed for management. Multiphase CT scan and MRI are comparable in pre-operative diagnosis and staging. Additional modalities like EUS, IDUS, cholangioscopy and DWI are complementary. Surgery, wherever possible, is the only curative treatment available. Various percutaneous interventions are available including PTBD, stenting, intra-biliary palliation and PVE as either pre-operative or palliative procedure in such patients.

REFERENCES

1. **Friman S.** Cholangiocarcinoma--current treatment options. *Scand J Surg* 2011; **100**: 30-34 [PMID: 21491796]
2. **Bold RJ,** Goodnight JE. Hilar cholangiocarcinoma: surgical and endoscopic approaches. *Surg Clin North Am* 2004; **84**: 525-542 [PMID: 15062660 DOI: 10.1016/S0039-6109(03)00232-9]
3. **Patel T.** Worldwide trends in mortality from biliary tract malignancies. *BMC Cancer* 2002; **2**: 10 [PMID: 11991810 DOI: 10.1186/1471-2407-2-10]
4. **Suarez-Munoz MA,** Fernandez-Aguilar JL, Sanchez-Perez B, Perez-Daga JA, Garcia-Albiach B, Pulido-Roa Y, Marin-Camero N, Santoyo-Santoyo J. Risk factors and classifications of hilar cholangiocarcinoma. *World J Gastrointest Oncol* 2013; **5**: 132-138 [PMID: 23919107 DOI: 10.4251/wjgo.v5.i7.132]
5. **Nakeeb A,** Pitt HA, Sohn TA, Coleman J, Abrams RA, Piantadosi S, Hruban RH, Lillemoe KD, Yeo CJ, Cameron JL. Cholangiocarcinoma. A spectrum of intrahepatic, perihilar, and distal tumors. *Ann Surg* 1996; **224**: 463-473; discussion 473-475 [PMID: 8857851 DOI: 10.1097/0000658-199610000-00005]
6. **DeOliveira ML,** Cunningham SC, Cameron JL, Kamangar F, Winter JM, Lillemoe KD, Choti MA, Yeo CJ, Schulick RD. Cholangiocarcinoma: thirty-one-year experience with 564 patients at a single institution. *Ann Surg* 2007; **245**: 755-762 [PMID: 17457168 DOI: 10.1097/01.sla.0000251366.62632.d3]

- 7 **Bismuth H**, Corlette MB. Intrahepatic cholangioenteric anastomosis in carcinoma of the hilus of the liver. *Surg Gynecol Obstet* 1975; **140**: 170-178 [PMID: 1079096]
- 8 **Bosman FT**, Carneiro F, Hruban RH, Theise ND. WHO classification of tumors of the digestive system. 4th ed. IARC: Lyon, 2010: 195-278
- 9 **Castellano-Megías VM**, Ibarrola-de Andrés C, Colina-Ruizdelgado F. Pathological aspects of so called "hilar cholangiocarcinoma". *World J Gastrointest Oncol* 2013; **5**: 159-170 [PMID: 23919110 DOI: 10.4251/wjgo.v5.i7.159]
- 10 **Liver Cancer Study Group of Japan**. The general rules for the clinical and pathological study of primary liver cancer, 4th ed. Tokyo: Kanehara, 2000
- 11 **Lim JH**, Park CK. Pathology of cholangiocarcinoma. *Abdom Imaging* 2004; **29**: 540-547 [PMID: 15383897 DOI: 10.1007/s00261-004-0187-2]
- 12 **Shin HR**, Oh JK, Masuyer E, Curado MP, Bouvard V, Fang YY, Wiangnon S, Sripa B, Hong ST. Epidemiology of cholangiocarcinoma: an update focusing on risk factors. *Cancer Sci* 2010; **101**: 579-585 [PMID: 20085587 DOI: 10.1111/j.1349-7006.2009.01458.x]
- 13 **Park HS**, Lee JM, Choi JY, Lee MW, Kim HJ, Han JK, Choi BI. Preoperative evaluation of bile duct cancer: MRI combined with MR cholangiopancreatography versus MDCT with direct cholangiography. *AJR Am J Roentgenol* 2008; **190**: 396-405 [PMID: 18212225 DOI: 10.2214/AJR.07.2310]
- 14 **Bloom CM**, Langer B, Wilson SR. Role of US in the detection, characterization, and staging of cholangiocarcinoma. *Radiographics* 1999; **19**: 1199-1218 [PMID: 10489176 DOI: 10.1148/radiographics.19.5.g99se081199]
- 15 **Hann LE**, Greatrex KV, Bach AM, Fong Y, Blumgart LH. Cholangiocarcinoma at the hepatic hilus: sonographic findings. *AJR Am J Roentgenol* 1997; **168**: 985-989 [PMID: 9124155 DOI: 10.2214/ajr.168.4.9124155]
- 16 **Choi BI**, Lee JH, Han MC, Kim SH, Yi JG, Kim CW. Hilar cholangiocarcinoma: comparative study with sonography and CT. *Radiology* 1989; **172**: 689-692 [PMID: 2549565 DOI: 10.1148/radiology.172.3.2549565]
- 17 **Neumaier CE**, Bertolotto M, Perrone R, Martinoli C, Loria F, Silvestri E. Staging of hilar cholangiocarcinoma with ultrasound. *J Clin Ultrasound* 1995; **23**: 173-178 [PMID: 7730463 DOI: 10.1002/jcu.1870230305]
- 18 **Xu HX**. Contrast-enhanced ultrasound in the biliary system: Potential uses and indications. *World J Radiol* 2009; **1**: 37-44 [PMID: 21160719 DOI: 10.4329/wjrv.v1.i1.37]
- 19 **Xu HX**, Chen LD, Xie XY, Xie XH, Xu ZF, Liu GJ, Lin MX, Wang Z, Lu MD. Enhancement pattern of hilar cholangiocarcinoma: contrast-enhanced ultrasound versus contrast-enhanced computed tomography. *Eur J Radiol* 2010; **75**: 197-202 [PMID: 19464836 DOI: 10.1016/j.ejrad.2009.04.060]
- 20 **Khalili K**, Metser U, Wilson SR. Hilar biliary obstruction: preliminary results with Levovist-enhanced sonography. *AJR Am J Roentgenol* 2003; **180**: 687-693 [PMID: 12591675 DOI: 10.2214/ajr.180.3.1800687]
- 21 **Aljiffry M**, Walsh MJ, Molinari M. Advances in diagnosis, treatment and palliation of cholangiocarcinoma: 1990-2009. *World J Gastroenterol* 2009; **15**: 4240-4262 [PMID: 19750567 DOI: 10.3748/wjg.15.4240]
- 22 **Mohamadnejad M**, DeWitt JM, Sherman S, LeBlanc JK, Pitt HA, House MG, Jones KJ, Fogel EL, McHenry L, Watkins JL, Cote GA, Lehman GA, Al-Haddad MA. Role of EUS for preoperative evaluation of cholangiocarcinoma: a large single-center experience. *Gastrointest Endosc* 2011; **73**: 71-78 [PMID: 21067747 DOI: 10.1016/j.gie.2010.08.050]
- 23 **Brugge WR**. Advances in the endoscopic management of patients with pancreatic and biliary malignancies. *South Med J* 2006; **99**: 1358-1366 [PMID: 17233192 DOI: 10.1097/01.smj.0000251324.81191.cd]
- 24 **Chak A**, Catanzaro A. Innovative methods of biliary tract diagnosis: intraductal ultrasound and tissue acquisition. *Gastrointest Endosc Clin N Am* 2003; **13**: 609-622 [DOI: 10.1016/S1052-5157(03)00068-0]
- 25 **Farrell RJ**, Agarwal B, Brandwein SL, Underhill J, Chuttani R, Pleskow DK. Intraductal US is a useful adjunct to ERCP for distinguishing malignant from benign biliary strictures. *Gastrointest Endosc* 2002; **56**: 681-687 [PMID: 12397276 DOI: 10.1016/S0016-5107(02)70117-X]
- 26 **Ahmetoğlu A**, Koşucu P, Kul S, Dinç H, Sari A, Arslan M, Alhan E, Gümele HR. MDCT cholangiography with volume rendering for the assessment of patients with biliary obstruction. *AJR Am J Roentgenol* 2004; **183**: 1327-1332 [PMID: 15505298 DOI: 10.2214/ajr.183.5.1831327]
- 27 **Cha JH**, Han JK, Kim TK, Kim AY, Park SJ, Choi BI, Suh KS, Kim SW, Han MC. Preoperative evaluation of Klatskin tumor: accuracy of spiral CT in determining vascular invasion as a sign of unresectability. *Abdom Imaging* 2000; **25**: 500-507 [PMID: 10931985 DOI: 10.1007/s002610000081]
- 28 **Ruys AT**, van Beem BE, Engelbrecht MR, Bipat S, Stoker J, Van Gulik TM. Radiological staging in patients with hilar cholangiocarcinoma: a systematic review and meta-analysis. *Br J Radiol* 2012; **85**: 1255-1262 [PMID: 22919007 DOI: 10.1259/bjr/88405305]
- 29 **Choi JY**, Kim MJ, Lee JM, Kim KW, Lee JY, Han JK, Choi BI. Hilar cholangiocarcinoma: role of preoperative imaging with sonography, MDCT, MRI, and direct cholangiography. *AJR Am J Roentgenol* 2008; **191**: 1448-1457 [PMID: 18941084 DOI: 10.2214/AJR.07.3992]
- 30 **Ramiah JM**. Hilar cholangiocarcinoma. *World J Gastrointest Oncol* 2013; **5**: 113-114 [PMID: 23919104 DOI: 10.4251/wjgo.v5.i7.115]
- 31 **Lim JH**. Cholangiocarcinoma: morphologic classification according to growth pattern and imaging findings. *AJR Am J Roentgenol* 2003; **181**: 819-827 [PMID: 12933488 DOI: 10.2214/ajr.181.3.1810819]
- 32 **Lee MG**, Lee HJ, Kim MH, Kang EM, Kim YH, Lee SG, Kim PN, Ha HK, Auh YH. Extrahepatic biliary diseases: 3D MR cholangiopancreatography compared with endoscopic retrograde cholangiopancreatography. *Radiology* 1997; **202**: 663-669 [PMID: 9051013 DOI: 10.1148/radiology.202.3.9051013]
- 33 **Kim HJ**, Lee JM, Kim SH, Han JK, Lee JY, Choi JY, Kim KH, Kim JY, Lee MW, Kim SJ, Choi BI. Evaluation of the longitudinal tumor extent of bile duct cancer: value of adding gadolinium-enhanced dynamic imaging to unenhanced images and magnetic resonance cholangiography. *J Comput Assist Tomogr* 2007; **31**: 469-474 [PMID: 17538298 DOI: 10.1097/01.rct.0000238011.42060.b5]
- 34 **Cui XY**, Chen HW. Role of diffusion-weighted magnetic resonance imaging in the diagnosis of extrahepatic cholangiocarcinoma. *World J Gastroenterol* 2010; **16**: 3196-3201 [PMID: 20593506 DOI: 10.3748/wjg.v16.i25.3196]
- 35 **Li N**, Liu C, Bi W, Lin X, Jiao H, Zhao P. MRCP and 3D LAVA imaging of extrahepatic cholangiocarcinoma at 3 T MRI. *Clin Radiol* 2012; **67**: 579-586 [PMID: 22137873 DOI: 10.1016/j.crad.2011.10.016]
- 36 **Jadvar H**, Henderson RW, Conti PS. [F-18]fluorodeoxyglucose positron emission tomography and positron emission tomography: computed tomography in recurrent and metastatic cholangiocarcinoma. *J Comput Assist Tomogr* 2007; **31**: 223-228 [PMID: 17414758 DOI: 10.1097/01.rct.0000237811.88251.d7]
- 37 **Kim JY**, Kim MH, Lee TY, Hwang CY, Kim JS, Yun SC, Lee SS, Seo DW, Lee SK. Clinical role of 18F-FDG PET-CT in suspected and potentially operable cholangiocarcinoma: a prospective study compared with conventional imaging. *Am J Gastroenterol* 2008; **103**: 1145-1151 [PMID: 18177454 DOI: 10.1111/j.1572-0241.2007.01710.x]
- 38 **Moon CM**, Bang S, Chung JB, Park SW, Song SY, Yun M, Lee JD. Usefulness of 18F-fluorodeoxyglucose positron emission tomography in differential diagnosis and staging of cholangiocarcinomas. *J Gastroenterol Hepatol* 2008; **23**: 759-765 [PMID: 17931372 DOI: 10.1111/j.1440-1746.2007.05173.x]
- 39 **Han JK**, Choi BI, Kim AY, An SK, Lee JW, Kim TK, Kim SW. Cholangiocarcinoma: pictorial essay of CT and cholangiographic findings. *Radiographics* 2002; **22**: 173-187 [PMID: 11796906 DOI: 10.1148/radiographics.22.1.g02ja15173]
- 40 **Nimura Y**. Staging cholangiocarcinoma by cholangioscopy. *HPB (Oxford)* 2008; **10**: 113-115 [PMID: 18773067 DOI: 10.1080/13651820801992658]
- 41 **Bismuth H**, Castaing D, Traynor O. Resection or palliation: priority of surgery in the treatment of hilar cancer. *World J Surg* 1988; **12**: 39-47

- [PMID: 2449769 DOI: 10.1007/BF01658484]
- 42 **Vogl TJ**, Schwarz WO, Heller M, Herzog C, Zangos S, Hintze RE, Neuhaus P, Hammerstingl RM. Staging of Klatskin tumours (hilar cholangiocarcinomas): comparison of MR cholangiography, MR imaging, and endoscopic retrograde cholangiography. *Eur Radiol* 2006; **16**: 2317-2325 [PMID: 16622690 DOI: 10.1007/s00330-005-0139-4]
 - 43 **Jarnagin WR**, Fong Y, DeMatteo RP, Gonen M, Burke EC, Bodniewicz BS J, Youssef BA M, Klimstra D, Blumgart LH. Staging, resectability and outcome in 225 patients with hilar cholangiocarcinoma. *Annals of Surgery* 2001; **234**: 507-519 [PMID: 11573054]
 - 44 **Edge SB**, Byrd DR, Compton CC, Fritz AG, Greene FL, Trotti A, editors. Perihilar bile ducts. AJCC Cancer Staging Manual. 7th ed. New York, NY: Springer, 2010: 219-222
 - 45 **Kloek JJ**, van der Gaag NA, Aziz Y, Rauws EA, van Delden OM, Lameris JS, Busch OR, Gouma DJ, van Gulik TM. Endoscopic and percutaneous preoperative biliary drainage in patients with suspected hilar cholangiocarcinoma. *J Gastrointest Surg* 2010; **14**: 119-125 [PMID: 19756881 DOI: 10.1007/s11605-009-1009-1]
 - 46 **Indar AA**, Lobo DN, Gilliam AD, Gregson R, Davidson I, Whittaker S, Doran J, Rowlands BJ, Beckingham IJ. Percutaneous biliary metal wall stenting in malignant obstructive jaundice. *Eur J Gastroenterol Hepatol* 2003; **15**: 915-919 [PMID: 12867803 DOI: 10.1097/00042737-200308000-00013]
 - 47 **George C**, Byass OR, Cast JE. Interventional radiology in the management of malignant biliary obstruction. *World J Gastrointest Oncol* 2010; **2**: 146-150 [PMID: 21160822 DOI: 10.4251/wjgo.v2.i3.146]
 - 48 **Chang WH**, Kortan P, Haber GB. Outcome in patients with bifurcation tumors who undergo unilateral versus bilateral hepatic duct drainage. *Gastrointest Endosc* 1998; **47**: 354-362 [PMID: 9609426 DOI: 10.1016/S0016-5107(98)70218-4]
 - 49 **van Delden OM**, Laméris JS. Percutaneous drainage and stenting for palliation of malignant bile duct obstruction. *Eur Radiol* 2008; **18**: 448-456 [PMID: 17960388 DOI: 10.1007/s00330-007-0796-6]
 - 50 **Küçükay F**, Okten RS, Yurdakul M, Ozdemir E, Parlak E, Olçer T, Cumhur T. Percutaneous management of malignant biliary disease: factors influencing the ability to overcome the stricture. *Diagn Interv Radiol* 2011; **17**: 169-173 [PMID: 20698007]
 - 51 **Mueller PR**, van Sonnenberg E, Ferrucci JT. Percutaneous biliary drainage: technical and catheter-related problems in 200 procedures. *AJR Am J Roentgenol* 1982; **138**: 17-23 [PMID: 6976698 DOI: 10.2214/ajr.138.1.17]
 - 52 **Xing GS**, Geng JC, Han XW, Dai JH, Wu CY. Endobiliary brush cytology during percutaneous transhepatic cholangiodrainage in patients with obstructive jaundice. *Hepatobiliary Pancreat Dis Int* 2005; **4**: 98-103 [PMID: 15730930]
 - 53 **Inal M**, Akgül E, Aksungur E, Demiryürek H, Yağmur O. Percutaneous self-expandable uncovered metallic stents in malignant biliary obstruction. Complications, follow-up and reintervention in 154 patients. *Acta Radiol* 2003; **44**: 139-146 [PMID: 12694096 DOI: 10.1034/j.1600-0455.2003.00049.x]
 - 54 **Lammer J**, Hausegger KA, Flückiger F, Winkelbauer FW, Wildling R, Klein GE, Thurnher SA, Havelec L. Common bile duct obstruction due to malignancy: treatment with plastic versus metal stents. *Radiology* 1996; **201**: 167-172 [PMID: 8816539 DOI: 10.1148/radiology.201.1.8816539]
 - 55 **Cho JH**, Jeon TJ, Park JY, Kim HM, Kim YJ, Park SW, Chung JB, Song SY, Bang S. Comparison of outcomes among secondary covered metallic, uncovered metallic, and plastic biliary stents in treating occluded primary metallic stents in malignant distal biliary obstruction. *Surg Endosc* 2011; **25**: 475-482 [PMID: 20602138 DOI: 10.1007/s00464-010-1196-6]
 - 56 **Hatzidakis A**, Krokidis M, Kalbakis K, Romanos J, Petrakis I, Gourtsoyannis N. ePTFE/FEP-covered metallic stents for palliation of malignant biliary disease: can tumor ingrowth be prevented? *Cardiovasc Intervent Radiol* 2007; **30**: 950-958 [PMID: 17508236 DOI: 10.1007/s00270-007-9049-y]
 - 57 **Killeen RP**, Harte S, Maguire D, Malone DE. Achievable outcomes in the management of proximal cholangiocarcinoma: an update prepared using "evidence-based practice" techniques. *Abdom Imaging* 2008; **33**: 54-57 [PMID: 17874306 DOI: 10.1007/s00261-007-9312-3]
 - 58 **Andrašina T**, Válek V, Pánek J, Kala Z, Kiss I, Tuček S, Slampa P. Multimodal oncological therapy comprising stents, brachytherapy, and regional chemotherapy for cholangiocarcinoma. *Gut Liver* 2010; **4** Suppl 1: S82-S88 [PMID: 21103300 DOI: 10.5009/gnl.2010.4.S1.S82]
 - 59 **Chen Y**, Wang XL, Yan ZP, Cheng JM, Wang JH, Gong GQ, Qian S, Luo JJ, Liu QX. HDR-192Ir intraluminal brachytherapy in treatment of malignant obstructive jaundice. *World J Gastroenterol* 2004; **10**: 3506-3510 [PMID: 15526374]
 - 60 **Lee TY**, Cheon YK, Shim CS, Cho YD. Photodynamic therapy prolongs metal stent patency in patients with unresectable hilar cholangiocarcinoma. *World J Gastroenterol* 2012; **18**: 5589-5594 [PMID: 23112552 DOI: 10.3748/wjg.v18.i39.5589]
 - 61 **Steel AW**, Postgate AJ, Khorsandi S, Nicholls J, Jiao L, Vlavianos P, Habib N, Westaby D. Endoscopically applied radiofrequency ablation appears to be safe in the treatment of malignant biliary obstruction. *Gastrointest Endosc* 2011; **73**: 149-153 [PMID: 21184881 DOI: 10.1016/j.gie.2010.09.031]
 - 62 **Fan WJ**, Wu PH, Zhang L, Huang JH, Zhang FJ, Gu YK, Zhao M, Huang XL, Guo CY. Radiofrequency ablation as a treatment for hilar cholangiocarcinoma. *World J Gastroenterol* 2008; **14**: 4540-4545 [PMID: 18680236 DOI: 10.3748/wjg.14.4540]
 - 63 **Alis H**, Sengoz C, Gonenc M, Kalayci MU, Kocatas A. Endobiliary radiofrequency ablation for malignant biliary obstruction. *Hepatobiliary Pancreat Dis Int* 2013; **12**: 423-427 [PMID: 23924501 DOI: 10.1016/S1499-3872(13)60066-1]
 - 64 **Giraud G**, Greget M, Oussoultzoglou E, Rosso E, Bachellier P, Jaeck D. Preoperative contralateral portal vein embolization before major hepatic resection is a safe and efficient procedure: a large single institution experience. *Surgery* 2008; **143**: 476-482 [PMID: 18374044 DOI: 10.1016/j.surg.2007.12.006]
 - 65 **May BJ**, Madoff DC. Portal vein embolization: rationale, technique, and current application. *Semin Intervent Radiol* 2012; **29**: 81-89 [PMID: 23729977 DOI: 10.1055/s-0032-1312568]
 - 66 **van Lienden KP**, van den Esschert JW, de Graaf W, Bipat S, Lameris JS, van Gulik TM, van Delden OM. Portal vein embolization before liver resection: a systematic review. *Cardiovasc Intervent Radiol* 2013; **36**: 25-34 [PMID: 22806245 DOI: 10.1007/s00270-012-0440-y]

P- Reviewer: Cerwenka HR, Verma S, Vinh-Hung V
S- Editor: Tian YL **L- Editor:** A **E- Editor:** Wu HL



Basic Study

Evaluation of changes of intracranial blood flow after carotid artery stenting using digital subtraction angiography flow assessment

Hajime Wada, Masato Saito, Kyousuke Kamada

Hajime Wada, Masato Saito, Kyousuke Kamada, Department of Neurosurgery, Asahikawa Medical University, Asahikawa, Hokkaido 0788510, Japan

Author contributions: All authors contributed to this work.

Ethics approval: The study was reviewed and approved.

Institutional animal care and use committee: This study has been approved by institutional ethical committee (No. 132).

Conflict-of-interest: The authors report no conflict of interest regarding the manuscript.

Data sharing: The authors accept the data sharing.

Open-Access: This article is an open-access article which was selected by an in-house editor and fully peer-reviewed by external reviewers. It is distributed in accordance with the Creative Commons Attribution Non Commercial (CC BY-NC 4.0) license, which permits others to distribute, remix, adapt, build upon this work non-commercially, and license their derivative works on different terms, provided the original work is properly cited and the use is non-commercial. See: <http://creativecommons.org/licenses/by-nc/4.0/>

Correspondence to: Kyousuke Kamada, MD, PhD, Department of Neurosurgery, Asahikawa Medical University, 2-1, 1-1, Midorigaoka-Higashi, Asahikawa, Hokkaido 078-8510, Japan. hjwada@asahikawa-med.ac.jp

Telephone: +81-166-682594

Fax: +81-166-682599

Received: October 28, 2014

Peer-review started: October 29, 2014

First decision: December 12, 2014

Revised: December 25, 2014

Accepted: January 15, 2015

Article in press: January 19, 2015

Published online: February 28, 2015

METHODS: Twenty patients treated by CAS participated in this study. We analyzed the change in concentration of the contrast media at the anterior-posterior and profile view image with the flow assessment application "Flow-Insight". And we compared the results with N-isopropyl-p-[123I] iodoamphetamine-single-photon emission computed tomography (IMP SPECT) performed before and after the treatment.

RESULTS: From this study, 200% of the parameter "blood flow" change in the post/pre-treatment is suggested as the critical line of the hyperperfusion syndrome arise. Although the observed blood flow increase in the digital subtraction angiography system did not strongly correlate with the rate of increase of SPECT, the "Flow-Insight" reflected the rate of change of the vessels well. However, for patients with reduced reserve blood flow before CAS, a highly elevated site was in agreement with the site analysis results.

CONCLUSION: We concluded that the cerebral angiography flow assessment application was able to more finely reveal hyperperfusion regions in the brain after CAS compared to SPECT.

Key words: Intracranial blood flow; Cerebral angiography; Carotid artery stenting; Single-photon emission computed tomography

© **The Author(s) 2015.** Published by Baishideng Publishing Group Inc. All rights reserved.

Abstract

AIM: To evaluate the changes of intracranial blood flow after carotid artery stenting (CAS), using the flow assessment application "Flow-Insight", which was developed in our department.

Core tip: Hyperperfusion syndrome is a relatively rare, but potentially serious, complication of carotid revascularization procedures. It is important to detect the excessive increase blood flow after treatment as soon as possible. We found that, although the observed blood flow increase in the digital subtraction

angiography system did not strongly correlate with the rate of increase of single-photon emission computed tomography before and after carotid artery stenting, the digital subtraction angiography flow assessment application more finely reflected the rate of change of the vessels well.

Wada H, Saito M, Kamada K. Evaluation of changes of intracranial blood flow after carotid artery stenting using digital subtraction angiography flow assessment. *World J Radiol* 2015; 7(2): 45-51 Available from: URL: <http://www.wjgnet.com/1949-8470/full/v7/i2/45.htm> DOI: <http://dx.doi.org/10.4329/wjr.v7.i2.45>

INTRODUCTION

Cerebral hyperperfusion after carotid revascularization treatment is defined as a major increase in ipsilateral cerebral blood flow (CBF) well above the metabolic demands of the brain tissue. Cerebral hyperperfusion syndrome is characterized by a unilateral headache, face and eye pain, seizures, and focal symptoms secondary to cerebral edema or intracerebral hemorrhage. The pathological mechanisms of the irreversible changes have been theorized to involve organic dysautoregulation of maximally dilated cerebral vessels. Although the incidence of intracerebral hemorrhage is relatively low, the prognosis for patients with this condition is poor^[1,2]. Schroeder *et al*^[3] reported that CBF on N-isopropyl-p-[123I] iodoamphetamine-single-photon emission computed tomography ([123I] IMP-SPECT) postoperatively is increased beyond that in the preoperative state^[3]; and, in cases of marked hypoperfusion, hyperperfusion after surgical revascularization is known to occur^[4].

In this study, we aimed to evaluate the change of intracranial blood flow after carotid artery stenting (CAS) using the flow assessment application "Flow-Insight," which was developed in our department; and to compare the results with those of IMP-SPECT, which is currently commonly used in clinical practice^[5].

MATERIALS AND METHODS

A total of 20 patients (18 men and 2 women), aged 56-82 years (mean, 70.0 ± 5.9 years), without large cortical infarction on conventional magnetic resonance imaging, who underwent CAS between October 2012 and April 2014 were enrolled in the present study. The mean degree of internal carotid artery stenosis was 75.3% ± 15.8% (range, 59%-93%), according to the method of the North American Symptomatic Carotid Endarterectomy Trial^[6]. Three patients had symptomatic stenosis and 4 patients had occlusion or stenosis greater

than 50% in the contralateral internal carotid artery. All cases of CAS were performed under general anesthesia, using a proximal balloon, distal filter protection, and flow reverse to the femoral vein. Using the location memory of the digital subtraction angiography (DSA) suit Artis zee (Siemens AG Healthcare, Erlangen, Germany), intracranial angiography acquisitions were evaluated in the same position before and after treatment. We analyzed the changes in the concentration of the contrast media as changes in brightness using the novel flow assessment application "Flow-Insight" (Infocom, Tokyo, Japan). The result images were created as an anterior-posterior (AP) view and a profile image. The software converts DSA DICOM image data to 8 bit digital data. It utilizes a mutual information method and phase correction of the two-dimensional Fourier transformation as a motion artifact correction method, and can calculate the integral value of the luminance change of each pixel in the converted data and the peak periods to examine. The calculated parameters include the calculation amount arrival time, time to peak, and mean transit time, with a focus on the time and blood volume, as determined by the accumulated amount of brightness and blood flow. In the result images, the rate of the blood flow is displayed by a color bar representing changes of 50%-200%. In this study, we used paired *t* test for parameter changes before and after CAS and statistical significance was less than 0.05. We determined the region of interest (ROI) in the result images, and compared the results by the ARG method with one 123I-IMP SPECT before and after CAS, using Spearman's rank correlation coefficient and simple regression analyses.

Statistical analysis

The study protocol was performed in accordance with the Declaration of Helsinki and its later amendments. All participants provided written informed consent.

RESULTS

Our results show that the novel "Flow-Insight" application was capable of determining a qualitative value of the blood flow, which was defined as the blood volume divided by the mean transit time (Figure 1B and C) using a central volume principle as previously described^[7]. The blood volume and mean transit time were determined using a time density curve (Figure 1A). We next created an ROI and calculated the cerebral blood flow before and after treatment, and compared the increased rate with the corresponding rate evaluated by IMP SPECT. The increased rate was calculated by taking the ratio of the cerebellum and the left and right blood flow communication. We found that the "Flow-Insight" blood flow increase rate of the middle cerebral artery

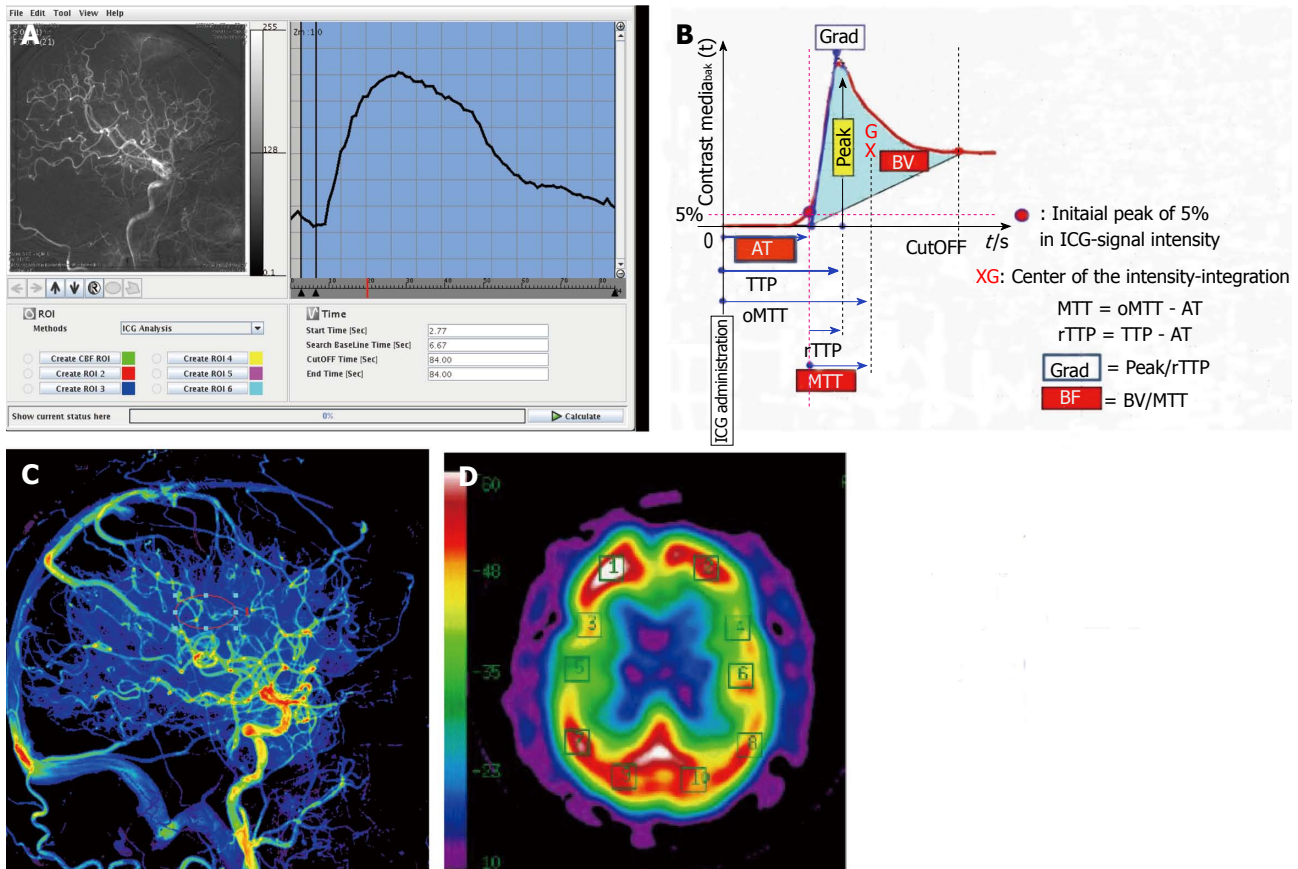


Figure 1 Digital subtraction angiography. A: Time-density curve of digital subtraction angiography lateral view. The change in the concentration of the contrast media, visualized as a change in brightness, was calculated; B: The parameters calculable by the "Flow-Insight" application; C: Lateral view of a pre-operative qualitative image of cerebral blood flow in Case 2; D: Pre-operative N-isopropyl-p-[123I] iodoamphetamine-single-photon emission computed tomography image.

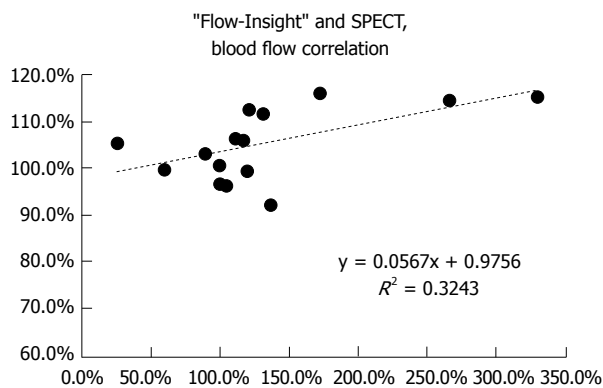


Figure 2 Horizontal axis: Rate of change of the "Flow-Insight" (%); Vertical axis: Rate of the rise of the ipsilateral cerebellum ratio as determined postoperatively by N-isopropyl-p-[123I] iodoamphetamine-single-photon emission computed tomography. SPECT: Single-photon emission computed tomography.

territory correlated with the increase ratio of the same SPECT territory in the cerebellum (Figure 2). The distribution with "Flow-Insight" was close to the 50%-200% range in all patients.

Because of the nature of DSA, it is generally difficult to capture the brain tissue blood perfusion changes. However, the images obtained using the "Flow-Insight" application were found to reflect the

changes in the vessels well. To avoid the vessels, we set the ROI as the motor and premotor cortex in the frontal lobe, just above the Sylvian fissure (Figure 1C and D). "Flow-Insight" successfully showed the highly elevated blood flow increase rate areas of patients with reduced vascular reserve areas.

In order to detect the actual increasing area in the human brain, we next created images based on the DSA blood flow increase ratio in the AP and lateral views, by dividing the post-operative CAS images by the pre-operative images (Figures 2 and 3). The result images showed the rate of blood flow, as defined by the color bar at 50%-200%. This range was chosen based on the range from the correlation of blood flow with SPECT. We reduced the image matrix settings to 100 × 100, because the displacement of high-resolution image calculations may lead to overestimation of the results.

It should be noted that the increased distribution observed after CAS was variable. For example, while Cases 1 and 2 did not show any blood flow from the contra-lateral *via* the anterior communicating artery, differences in the increased area and in the degree of the increase were noted upon DSA (Figure 3). Conversely, Cases 3 and 4 suffered severe right cervical internal carotid artery stenosis, and our

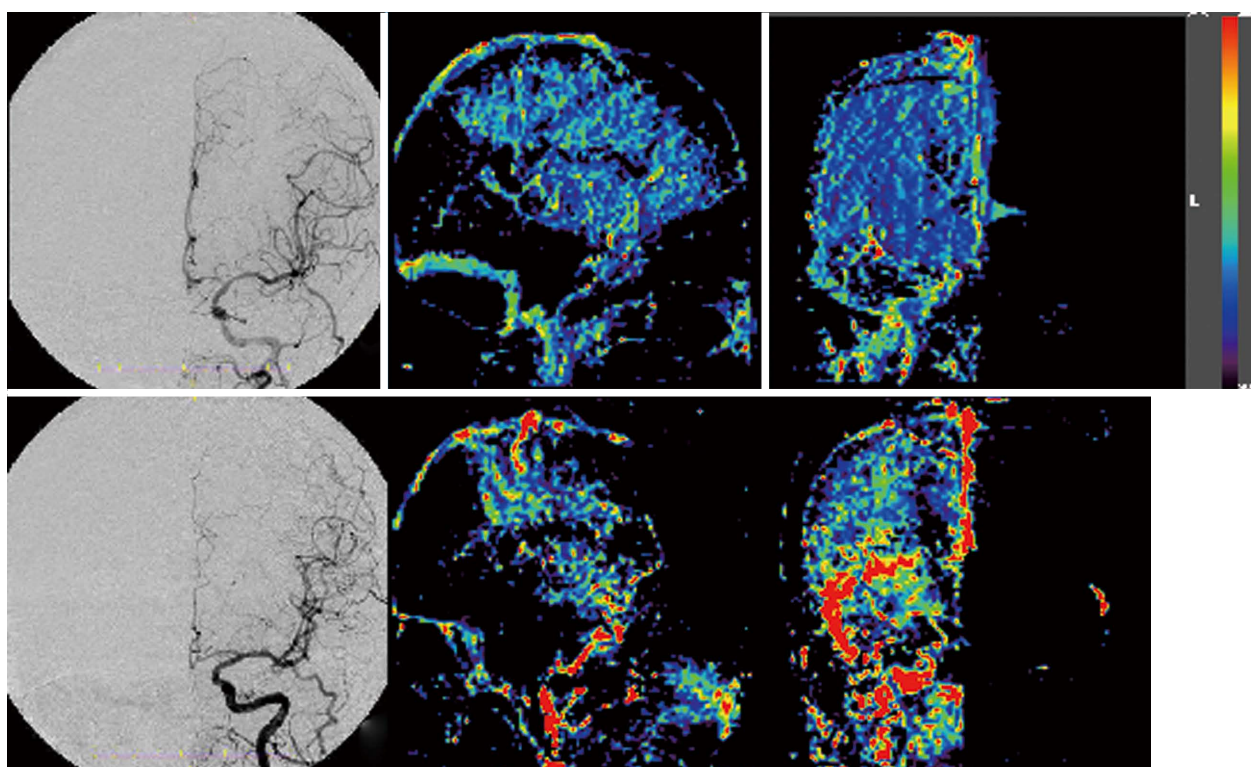


Figure 3 Upper panel: Digital subtraction angiography anterior-posterior view, lateral view showing the blood flow increase ratio, and the anterior-posterior view in Case 1; and Lower panel: Case 2, same series. Pre-operative digital subtraction angiography in Cases 1 and 2 did not reveal blood flow to the operative side *via* the anterior communicating artery. In Case 1, a wide and slight increase was noted in the area in the middle cerebral artery territory. In Case 2, the increase was only noted in a part of the middle cerebral artery perfusion area; the rate of increase was high.

analyses revealed blood flow from the contra-lateral side *via* the anterior communicating artery at the preoperative DSA (Figure 4). However, while the SPECT for case 4 showed a 114.2% increase ratio, the “Flow-Insight” showed a 265% increase ratio. The patient suffered mild delirium symptoms for 2 d after CAS. On the other hand, Case 3 also showed blood flow *via* the anterior communicating artery. However, in this case, the “Flow-Insight” blood flow increase ratio was only 131%, while the SPECT also showed a relatively low ratio, at 111.3%, suggesting that the patient did not suffer hyper-perfusion syndrome *per se*. The fact that the distribution of the intracranial blood flow increase rate after CAS showed quite different results in each case, not only in terms of the presence or absence of the left and right or anterior-posterior communication, but also in terms of the diameter and length, may be due to differences in the degree and area of the increased blood flow. The “Flow-Insight” application successfully revealed the presence of increased blood flow regions, which were not evident upon conventional SPECT.

DISCUSSION

In the case of carotid endarterectomy, the presence or absence of collateral flow *via* the anterior or posterior communicating artery deeply affects the

risk of intraoperative ischemic complications^[8,9]. Moreover, intraoperative measurement of distal internal carotid artery pressure reflects the intracranial vascular reserve, and is important in predicting postoperative hyperperfusion^[4]. Reduced blood flow due to internal carotid artery stenosis results in decreased blood flow reserves intracranially, and this has been demonstrated to be significantly influenced by the microscopic vascular bed and the left and right or anterior and posterior communication^[10]. Local increases of blood flow after treatment and blood flow buffering through the left-right or anterior-posterior communication may lead to hyperperfusion syndrome. Therefore, hyperperfusion syndrome cannot completely be predicted by the presence or absence of blood flow communication only. Furthermore, local variations at the site of the blood flow increase may cause different symptoms of hyperperfusion syndrome, such as headaches, intracranial hemorrhage (subarachnoid hemorrhage, subcortical hemorrhage, or basal ganglia hemorrhage), delirium, or convulsions^[1,2,11].

IMP-SPECT is currently the conventional modality for measuring intracranial blood flow. In this study, when comparing the SPECT and the “Flow-Insight” blood flow increase rates in the whole treated area, no clear correlation was observed. However, when evaluating the correlation restricted to the MCA territory, which is devoid of major vessels and which

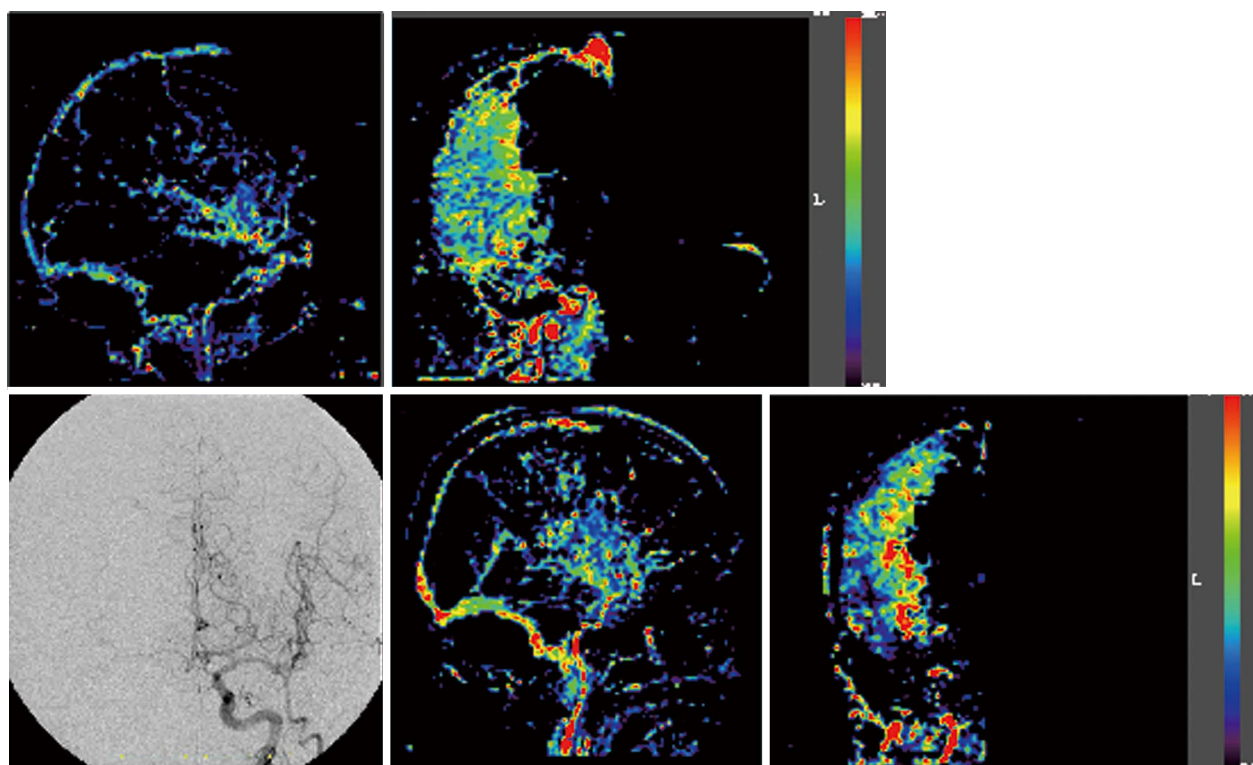


Figure 4 Upper panel: Digital subtraction angiography anterior-posterior view, lateral view showing the blood flow increase ratio, and the anterior-posterior view in Case 3; and Lower panel: Case 4, same series. Pre-operative digital subtraction angiography in Cases 3 and 4 revealed blood flow to the operative side via the anterior communicating artery. A wide and uniform increase in the area in the middle cerebral artery territory was noted in Case 3. In Case 4, the increase was only noted in a part of the middle cerebral artery perfusion area, especially in the basal ganglia; the rate of increase was high.

is the perfusion area of the internal carotid artery, we detected a good correlation. We moreover found that increased blood flow after treatment of internal carotid artery stenosis is not confined to a uniform territory. However, we were unable to draw any firm and conclusions regarding this observation because of the limited size of the study, since only one patient presented with typical hyperperfusion syndrome. This novel evaluation method revealed the increase ratio and its intracranial distribution, and because it strongly reflected the local vascular reserve, as well as the left and right or anterior-posterior artery communication, we believe that it has the potential to predict the presence of hyperperfusion syndrome.

At this time, quantification of cerebral blood flow is not available from the "Flow-Insight". However, we hypothesized that if there was a high correlation with the results of the post-operative blood flow achieved from the "Flow-Insight" and that obtained from SPECT, the "Flow-Insight" would be able to predict post-operative hyperperfusion syndrome. Accordingly, we found that the "Flow-Insight" blood flow increase rate correlated with the increase ratio of SPECT. However, the correlation, R^2 , was 0.324, which suggests that the correlation was only moderate. One reason for why no strong correlation was observed could be that the "Flow-Insight" is performed immediately after treatment, whereas SPECT is usually performed approximately 24 h

post-operation. After CAS, normalization of cerebral blood flow may spontaneously be initiated. Thus, the results of the flow assessment using DSA will be different from the blood flow measured by SPECT in the following points: first, contrast medium is a non-diffusible tracer. The contrast medium is injected just proximal of the lesion in "Flow-Insight," indicating that this evaluation method is highly focal. Moreover, it is based on processing of an image acquired by the inhibition of the radiation translucency and subtraction of an X-ray image. Accordingly, "Flow-Insight" reveals slightly different blood flow from that evaluated by conventional SPECT or computed tomography perfusion. In terms of the terminology of this novel method, it should be pointed out that "Flow-Insight" is the flow assessment software used, while cerebral angiography is simply a method used to obtain the black-and-white 2D image, and is used only to evaluate the appearance of the vascular system, such as the form of aneurysms or continuity of vessels. However, a major advantage of DSA is that it has a time scale, which computed tomography angiography and magnetic resonance angiography do not.

It has been previously reported that the right and left venous phase appearance times are symmetrical in the internal carotid artery occlusion test (balloon occlusion test)^[12], and this method has been proposed as an alternative to angiographic imaging.

However, it was due to the statistical processing taking a partial ROI.

By using the "Flow-Insight" software, it is easy to visualize the intracranial blood flow changes using the color bar, despite the 2D nature of the images. It is hence a useful indicator to understand the entire brain, unlike focal methods evaluating only the ROI. Moreover, the fact that it can be used immediately after treatment unlike other post-operative evaluations such as SPECT or computed tomography perfusion is a great advantage.

Application of flow assessment angiography with indocyanine green in bypass surgery has been previously reported^[13-15], and cerebral blood flow assessment using the latest DSA system may also be applied for these patients^[16]. The "Flow-Insight" application is based on the same principle as flow assessment angiography and is easy to use with the proper equipment. However, the method of analysis could be improved further, and the application is currently inconvenient to apply in other ways. DSA flow assessment is also associated with a number of issues related to certain factors, such as the head position during data acquisition, the velocity and amount of contrast media used, and the diameter of the catheter. Moreover, it is a direct injection of contrast media, which may cause increased pressure in the arteries, rather than a systemic intravenous administration into the physiological blood flow. Furthermore, since it is based on two-dimensional images, the accumulated value of the 2D images are greatly affected by the three-dimensional volume, such as for example the intracranial venous phase overlapping with the arterial phase, and the image accumulated by subtraction images can be easily affected by motion artifacts. However, the risk of this can be minimized by using general anesthesia to keep the patients stationary, and by the angle and position of the table being memorized by a specialized device during the treatment. In the future, if it becomes possible to perform 3D assessment analyses, it can be expected that the accuracy of this application will dramatically improve.

In the present study, using flow assessment application we were able to reveal more finely hyperperfusion regions in the brain after CAS. Flow assessment application was useful for understanding the pathology of the brain post-CAS. Further studies to determine the optimal angiographic conditions, such as the optimal contrast agent concentration and amount, are warranted.

COMMENTS

Background

Flow assessment study derived from digital subtraction angiography (DSA) for the cerebral arterial flow in clinical settings have been proposed, but no exist so much. Hyperperfusion syndrome is a relatively rare, but potentially serious, complication of carotid artery stenting. Therefore, the authors applied to detect the excessive increase blood flow after treatment.

Research frontiers

In the present study, using flow assessment application of cerebral angiography the authors were able to reveal more finely hyperperfusion regions in the brain after carotid artery stenting. Then it suggests that any hyperperfusion syndrome variation is come from which brain area of excessive increased flow.

Innovations and breakthroughs

Just after treatment, only usual cerebral angiography, without using other modality, can predict the occurrence of serious complications. Furthermore, it reveals that flow assessment application was aim to be a useful clinical application.

Applications

From this study, 200% of the parameter "blood flow" change in the post/pre-treatment is suggested as the critical line of the hyperperfusion syndrome arise. By using the "Flow-Insight" software, it is easy to visualize the intracranial blood flow changes using the color bar, despite the 2D nature of the images. It is hence a useful indicator to understand the entire brain, unlike focal methods evaluating only the region of interest.

Terminology

Flow assessment application: It analyze focal blood flow and derive parametric imaging maps from DSA. The origin is from Indocyanine green video angiography at the open micro-surgery. Cerebral hyperperfusion syndrome: It is a rare, serious complication either after carotid endarterectomy or carotid stent placement. Impaired cerebral autoregulation. The syndrome is characterized by a unilateral headache, face and eye pain, seizures, and focal symptoms secondary to cerebral edema or intracerebral hemorrhage. It may be fatal once an intracranial hemorrhage occurs.

Peer-review

The paper is well written.

REFERENCES

- 1 **Bernstein M**, Fleming JF, Deck JH. Cerebral hyperperfusion after carotid endarterectomy: a cause of cerebral hemorrhage. *Neurosurgery* 1984; **15**: 50-56 [PMID: 6472594]
- 2 **Piegras DG**, Morgan MK, Sundt TM, Yanagihara T, Mussman LM. Intracerebral hemorrhage after carotid endarterectomy. *J Neurosurg* 1988; **68**: 532-536 [PMID: 3351580 DOI: 10.3171/jns.1988.68.4.0532]
- 3 **Schroeder T**, Sillesen H, Sørensen O, Engell HC. Cerebral hyperperfusion following carotid endarterectomy. *J Neurosurg* 1987; **66**: 824-829 [PMID: 3572512]
- 4 **Yoshimoto T**, Shirasaka T, Yoshizumi T, Fujimoto S, Kaneko S, Kashiwaba T. Evaluation of carotid distal pressure for prevention of hyperperfusion after carotid endarterectomy. *Surg Neurol* 2005; **63**: 554-557; discussion 557-558 [DOI: 10.1016/j.surneu.2004.06.016]
- 5 **Iida H**, Itoh H, Nakazawa M, Hatazawa J, Nishimura H, Onishi Y, Uemura K. Quantitative mapping of regional cerebral blood flow using iodine-123-IMP and SPECT. *J Nucl Med* 1994; **35**: 2019-2030 [PMID: 7989987]
- 6 **North American Symptomatic Carotid Endarterectomy Trial Collaborators**. Beneficial effect of carotid endarterectomy in symptomatic patients with high-grade carotid stenosis. *N Engl J Med* 1991; **325**: 445-453 [PMID: 1852179 DOI: 10.1056/NEJM199108153250701]
- 7 **Meier P**, Zierler KL. On the theory of the indicator-dilution method for measurement of blood flow and volume. *J Appl Physiol* 1954; **6**: 731-744 [PMID: 13174454]
- 8 **Lopez-Bresnahan MV**, Kears LA, Yanez P, Young TI. Anterior communicating artery collateral flow protection against ischemic change during carotid endarterectomy. *J Neurosurg* 1993; **79**: 379-382 [PMID: 8360734 DOI: 10.3171/jns.1993.79.3.0379]
- 9 **Schwartz RB**, Jones KM, LeClerc GT, Ahn SS, Chabot R, Whittemore A, Mannick JA, Donaldson MC, Gugino LD. The value of cerebral angiography in predicting cerebral ischemia during carotid endarterectomy. *AJR Am J Roentgenol* 1992; **159**: 1057-1061 [PMID: 1414775 DOI: 10.2214/ajr.159.5.1414775]
- 10 **Kuroda H**, Ogasawara K, Hirooka R, Kobayashi M, Fujiwara S, Chida K, Ishigaki D, Otawara Y, Ogawa A. Prediction of cerebral hyperperfusion after carotid endarterectomy using middle cerebral

- artery signal intensity in preoperative single-slab 3-dimensional time-of-flight magnetic resonance angiography. *Neurosurgery* 2009; **64**: 1065-1071; discussion 1071-1072 [PMID: 19487885 DOI: 10.1227/01.NEU.0000345941.99443.99]
- 11 **Solomon RA**, Loftus CM, Quest DO, Correll JW. Incidence and etiology of intracerebral hemorrhage following carotid endarterectomy. *J Neurosurg* 1986; **64**: 29-34 [PMID: 3941347 DOI: 10.3171/jns.1986.64.1.0029]
 - 12 **Abud DG**, Spelle L, Pötting M, Mounayer C, Vanzin JR, Moret J. Venous phase timing during balloon test occlusion as a criterion for permanent internal carotid artery sacrifice. *AJNR Am J Neuroradiol* 2005; **26**: 2602-2609 [PMID: 16286409]
 - 13 **Li J**, Lan Z, He M, You C. Assessment of microscope-integrated indocyanine green angiography during intracranial aneurysm surgery: a retrospective study of 120 patients. *Neurol India* 2009; **57**: 453-459 [PMID: 19770547 DOI: 10.4103/0028-3886.55607]
 - 14 **Oda J**, Kato Y, Chen SF, Sodhiya P, Watabe T, Imizu S, Oguri D, Sano H, Hirose Y. Intraoperative near-infrared indocyanine green-videoangiography (ICG-VA) and graphic analysis of fluorescence intensity in cerebral aneurysm surgery. *J Clin Neurosci* 2011; **18**: 1097-1100 [PMID: 21715173 DOI: 10.1016/j.jocn.2010.12.045]
 - 15 **Uchino H**, Nakamura T, Houkin K, Murata J, Saito H, Kuroda S. Semiquantitative analysis of indocyanine green videoangiography for cortical perfusion assessment in superficial temporal artery to middle cerebral artery anastomosis. *Acta Neurochir (Wien)* 2013; **155**: 599-605 [PMID: 23287901 DOI: 10.1007/s00701-012-1575-y]
 - 16 **Struffert T**, Deuerling-Zheng Y, Engelhorn T, Kloska S, Göllitz P, Bozzato A, Kapsreiter M, Strother CM, Doerfler A. Monitoring of balloon test occlusion of the internal carotid artery by parametric color coding and perfusion imaging within the angio suite: first results. *Clin Neuroradiol* 2013; **23**: 285-292 [PMID: 23525670 DOI: 10.1007/s00062-013-0208-z]

P- Reviewer: Rodriguez GJ, Spalice A, Shen J **S- Editor:** Ji FF
L- Editor: A **E- Editor:** Wu HL



Retrospective Study

Transcranial Doppler screening in sickle cell disease: The implications of using peak systolic criteria

Lena N Naffaa, Yasmeen K Tandon, Neville Irani

Lena N Naffaa, Department of Radiology, Akron Children's Hospital, Akron, OH 44308, United States

Yasmeen K Tandon, Department of Radiology, Case Western Reserve University-Metro Health Medical Center, Cleveland, OH 44109, United States

Neville Irani, Radiology, Kansas University Medical Center, Kansas City, KS 66160, United States

Author contributions: Naffaa LN, Tandon YK and Irani N contributed equally to this work; Naffaa LN and Irani N interpreted images in this study; Naffaa LN, Tandon YK and Irani N collected the patient's clinical data; Naffaa LN, Tandon YK and Irani N analyzed the data and wrote the paper; Naffaa LN, Tandon YK and Irani N gave final approval of the version to be published.

Ethics approval: The study was reviewed and approved by the Akron Children's Hospital Institutional Review Board.

Informed consent: Informed consent was not required for this study as it was a retrospective study and the presented data are anonymized and risk of identification is low.

Conflict-of-interest: The authors have no conflicts of interest to declare.

Data sharing: Technical appendix, statistical code, and dataset available from the corresponding author at lnaffaa@chmca.org.

Open-Access: This article is an open-access article which was selected by an in-house editor and fully peer-reviewed by external reviewers. It is distributed in accordance with the Creative Commons Attribution Non Commercial (CC BY-NC 4.0) license, which permits others to distribute, remix, adapt, build upon this work non-commercially, and license their derivative works on different terms, provided the original work is properly cited and the use is non-commercial. See: <http://creativecommons.org/licenses/by-nc/4.0/>

Correspondence to: Lena N Naffaa, MD, Radiologist, Department of Radiology, Akron Children's Hospital, 1 Perkins Square, Akron, OH 44308, United States. lnaffaa@chmca.org

Telephone: +1-330-5438275

Fax: +1-330-5433760

Received: October 14, 2014

Peer-review started: October 15, 2014

First decision: December 17, 2014

Revised: December 25, 2014

Accepted: January 18, 2015

Article in press: January 20, 2015

Published online: February 28, 2015

Abstract

AIM: To compare time average maximum mean velocity (TAMV) and peak systolic velocity (PSV) criteria of Trans Cranial Doppler (TCD) in their ability to predict abnormalities on magnetic resonance imaging (MRI)/magnetic resonance angiogram (MRA) in patients with sickle cell disease.

METHODS: A retrospective evaluation was performed of the outcomes in all patients with a Transcranial Doppler examination at our institution since the implementation of the hospital picture archiving and communication system (PACS) system in January 2003 through December 2012. All ultrasound imaging exams were performed by the same technologist with a 3 MHz transducer. Inclusion criteria was based upon the Transcranial Doppler procedure code in our PACS which had an indication of sickle cell disease in the history. The patient's age and gender along with the vessel with the highest time averaged mean velocity as well as the highest peak systolic velocity was recorded for analysis. A subset of the study cohort also had subsequent MR imaging and Angiograms performed within 6 mo of the TCD examination. MRI results were categorized as having a disease related abnormality (vessel narrowing, collateral formation/moya-moya, or abnormal fluid attenuation inversion recovery signal in parenchyma indicative of prior stroke) or normal. The MRI results formed the comparison standards for TCD exams in evaluating intracranial injury. Sensitivity and specificity for the two TCD criteria (TAMV and PSV) were calculated to determine which could be a better predictor for intracranial vasculopathy /clinically occult strokes.

RESULTS: The study cohort for our institution was 110

patients with a total of 291 TCD examinations. These patients had a mean age of 7.6 years with a range from 2-18 years of age. Sixty-two of the 110 patients (56%) had two or more TCD exams. Thirty-seven patients (34%) had at least one MRI following a TCD examination. Of the 291 TCD examinations, 46 (16%) were conditional or abnormal by TAMV criteria. One hundred and sixteen (40%) were conditional or abnormal by PSV criteria. All studies that were abnormal by TAMV were also abnormal by PSV criteria. Seventy of the 116 (60%) studies which were conditional or abnormal by peak systolic criteria would not have been identified by time averaged mean maximum velocity criteria. The most frequent location of highest velocity measurement was noted to be in the middle cerebral artery regardless of whether it was measured by PSV or TAMV. From the 37 patients having one or more MRIs, 43 MRI exams were performed within 6 mo of a TCD examination. Twenty two (51%) MRIs had a disease related abnormality reported. When evaluating conditional or abnormal exams by PSV criteria against follow-up MRI/MRA, the sensitivity was 73% [16/(16 + 6)] and specificity was 81% [17/(4 + 17)]. When evaluating conditional or abnormal exams by TAMV criteria by follow-up MRI/MRA as the gold standard, the sensitivity was 41% [9/(9 + 13)] and the specificity was 100% [21/(21 + 0)]. In using conditional or abnormal criteria from PSV and TAMV to predict abnormalities on follow-up MRI/MR Angiogram, PSV was more sensitive (73% *vs* 41%) while TAMV was more specific (100% *vs* 81%).

CONCLUSION: Based on the data obtained at our institution and using the assumption that the best screening test is the one with the highest sensitivity, the peak systolic velocity could be the measurement of choice for TCD screening.

Key words: Sickle; Ischemic; Stroke; Trans Cranial Doppler; Average maximum mean velocity; Peak systolic velocity; Magnetic resonance imaging

© The Author(s) 2015. Published by Baishideng Publishing Group Inc. All rights reserved.

Core tip: To the best of our knowledge, there has been no direct comparison between peak systolic velocity and time average maximum mean velocity in their ability to predict abnormalities on magnetic resonance imaging (MRI)/magnetic resonance angiogram in children with sickle cell disease. With the growing clinical use of MR Angiography to assess sickle cell patients, the sensitivity of Trans Cranial Doppler (TCD) should be maximized if it is to maintain its role as a screening test in the sickle cell population. Based on the data obtained at our institution and using the assumption that the best screening test is the one with the highest sensitivity, the peak systolic velocity could be the measurement of choice for TCD screening.

Naffaa LN, Tandon YK, Irani N. Transcranial Doppler screening in sickle cell disease: The implications of using peak systolic criteria. *World J Radiol* 2015; 7(2): 52-56 Available from: URL:

INTRODUCTION

Over the past 20 years, there has been a significant increase in understanding the cerebrovascular consequences of sickle cell disease. Without treatment, 11% of children with sickle cell disease will have an ischemic stroke by 20 years of age^[1]. It is also well documented that children with an ischemic stroke are at high risk for recurrence unless treated with repeated transfusions with a goal of maintaining the level of sickle hemoglobin below 30%^[2]. By treating the patients with abnormal time average maximum mean velocity (TAMV) with transfusion, the 10% per year risk of stroke is reduced to less than 1%^[3].

The Stroke Prevention Trial in Sickle Cell Anemia (STOP) was a significant advance in screening for this complication of sickle cell disease as it demonstrated the efficacy of Trans Cranial Doppler (TCD) in identifying patients at high risk for ischemic brain injury. The trial involved correlating the TAMV in the internal carotid artery (ICA) and proximal middle cerebral artery (MCA) on an annual Doppler waveform tracing with the clinical outcome of stroke. A TAMV of 200 cm/s was indicative of a 10% stroke risk over the ensuing year, while a level of 170 cm/s was considered conditional, requiring shorter interval follow-up^[3].

The thresholds that carried forward into the STOP trial grew from a post hoc analysis of potential cutoff values for TAMV which looked to minimize false positives and yield the highest relative risk. The analysis did not maximize sensitivity as would be assumed if the intent were to utilize this test to screen asymptomatic patients with sickle cell disease. This fundamental oversight in selecting the TAMV criteria ultimately undercuts TCD's potential as a screening test. The reference standard in evaluating thresholds in the 1992 analysis was cerebral angiography and not MRI; the latter is now the current standard of care for stroke detection. Indeed, in many centers, MRI is now ordered more frequently than TCD for sickle cell patients as reporting of TCD results based upon TAMV criteria do not satisfy the criteria of an optimal screening test. If we look back at the original data, the highest sensitivity for patients with stroke was not at 170 cm/s, but rather, at a much lower level of 140 cm/s. A final consideration in how this cutoff determination process ultimately limits TCD's applicability is the relatively small cohort of seven patients with clinically evident stroke that was included in the original analysis^[4].

In 2005, the results from the STOP trial were revisited to determine if another, equally predictive,

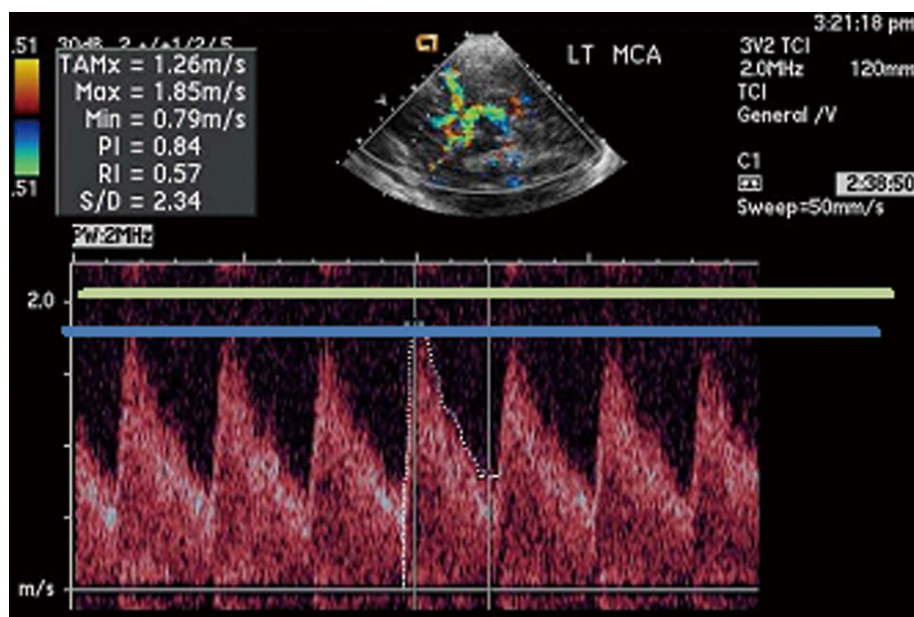


Figure 1 Example of time averaged mean maximum velocity measurement in the left middle cerebral artery. The green line represents the cutoff for PSV (200 cm/s) which was considered conditional requiring increased surveillance. The blue line represents the cutoff for TAMV (170 cm/s) which was considered conditional requiring increased surveillance. This study did not result in a conditional interpretation by either criteria (TAMV = 126 cm/s and PSV = 185 cm/s). MCA: Middle cerebral artery; TAMV: Time average maximum mean velocity; PSV: Peak systolic velocity.

criterion for clinically apparent stroke could be found for TCD with imaging acquisition (the more common TCD method utilized in practice for sickle cell patients). Peak systolic velocity (PSV) was one of the measures evaluated as it has long been a metric for determining stenosis in other important vascular distributions^[5]. A comparison of PSV and TAMV revealed that the PSV appeared to predict stroke as well as TAMV albeit with different velocity cutoffs. From this analysis, came the recommendation of using a PSV of 250 cm/s being as abnormal (high risk) and a PSV of 200 cm/s or greater considered conditional requiring increased surveillance^[6].

Following this analysis, there are now two possible criteria (PSV and TAMV) which validated against the same data set, as being equally predictive of a clinically apparent stroke. In practice, it would seem that the sensitivity of the TCD evaluation in predicting the more proximate cause of sickle cell stroke (intracranial vasculopathy) should depend upon which of these criteria were utilized to identify "normal". To our knowledge, there has been no comparison of these two criteria in their ability to predict abnormalities on MRI/MRA.

With the growing clinical use of magnetic resonance imaging (MRI)/magnetic resonance angiogram (MRA) to assess sickle cell patients, the sensitivity of TCD should be maximized if it is to maintain its role as a screening test in the sickle cell population. Our retrospective analysis of eight years of TCD data at our institution aims to provide this correlation.

MATERIALS AND METHODS

Our Institutional Review Board approved a retro-

spective evaluation of the outcomes in all patients with a Transcranial Doppler examination at our institution since the implementation of the hospital PACS system in January 2003 through December 2012. All ultrasound imaging exams were performed by the same technologist with a 3 MHz transducer. Inclusion criteria was based upon the Transcranial Doppler procedure code in our PACS which had an indication of sickle cell disease in the history. Indications other than sickle cell disease were excluded (e.g., ancillary brain death evaluation, vasospasm). The patient age and gender along with the vessel with the highest time averaged mean velocity as well as the highest peak systolic velocity was recorded for analysis (Figure 1).

A subset of the study cohort also had subsequent MR imaging and Angiograms performed within 6 mo of the TCD examination on a 1.5 Tesla MRI. MRI results were categorized as having a disease related abnormality (vessel narrowing, collateral formation/moya-moya, or abnormal fluid attenuation inversion recovery signal in parenchyma indicative of prior stroke) or normal. The MRI results formed the comparison standards for TCD exams in evaluating intracranial injury.

Sensitivity and specificity for the two TCD criteria (TAMV and PSV) were calculated to determine which could be a better predictor for intracranial vasculopathy /clinically occult strokes.

Statistical analysis

The statistics were reviewed and analyzed by the authors. Determinations of sensitivity and specificity were made based upon data collected and public domain information. No biostatistician was involved

Table 1 Evaluating Peak Systolic Criteria by follow-up magnetic resonance imaging/magnetic resonance angiogram

		MRI/MRA	
		Condition/ abnormal	Normal
Peak systolic criteria	Conditional/ abnormal	16	4
	Normal	6	17

The sensitivity was 73% [16/(16 + 6)] and specificity was 81% [17/(4 + 17)].
MRI: Magnetic resonance imaging; MRA: Magnetic resonance angiogram.

with this project due to resource constraints.

RESULTS

The study cohort for our institution was 110 patients with a total of 291 TCD examinations. These patients had a mean age of 7.6 years with a range from 2-18 years of age. Sixty-two of the 110 patients (56%) had two or more TCD exams. Thirty-seven patients (34%) had at least one MRI following a TCD examination. The subset of patients with an MRI exam following the TCD exam had a higher age, as expected, with a mean of 8.6 years with a range of 3-18 years.

Of the 291 TCD examinations, 46 (16%) were conditional or abnormal by TAMV criteria. One hundred and sixteen (40%) were conditional or abnormal by PSV criteria. All studies that were abnormal by TAMV were also abnormal by PSV criteria. Seventy of the 116 (60%) studies which were conditional or abnormal by peak systolic criteria would not have been identified by time averaged mean maximum velocity criteria.

The most frequent location of highest velocity measurement was noted to be in the MCA regardless of whether it was measured by PSV or TAMV. This accounted for over 80% of all exams during our study period. For TAMV measurement, the ACA demonstrated the highest velocity in 19% of exams. The highest PSV was found in the ACA in 16% of exams. One exam demonstrated the highest velocity within the PCA, although the TAMV and PSV were both less than 100 cm/s. No exams (using either criteria) found the highest velocity to be within the ICA.

From the 37 patients having one or more MRIs, 43 MRI exams were performed within 6 mo of a TCD examination. Twenty two (51%) MRIs had a disease related abnormality reported. When evaluating conditional or abnormal exams by PSV criteria against follow-up MRI/MRA (Table 1), the sensitivity was 73% [16/(16 + 6)] and specificity was 81% [17/(4 + 17)]. When evaluating conditional or abnormal exams by TAMV criteria by follow-up MRI/MRA as the gold standard (Table 2), the sensitivity was 41% [9/(9 + 9 + 13)] and the specificity

Table 2 Evaluating mean velocity criteria by follow-up magnetic resonance imaging/magnetic resonance angiogram

		MRI/MRA	
		Condition/ abnormal	Normal
Mean velocity criteria	Conditional/ abnormal	9	0
	Normal	13	21

The sensitivity was 41% [9/(9 + 9 + 13)] and the specificity was 100% [21/(21 + 0)]. MRI: Magnetic resonance imaging; MRA: Magnetic resonance angiogram.

was 100% [21/(21 + 0)]. In using conditional or abnormal criteria from PSV and TAMV to predict abnormalities on follow-up MRI/MR Angiogram, PSV was more sensitive (73% vs 41%) while TAMV was more specific (100% vs 81%).

DISCUSSION

Since the original STOP trial publication, there has been a significant increase in utilization of TCD with imaging in asymptomatic sickle cell patients to identify increased stroke risk^[7]. A finding of elevated velocities requires further monitoring or transfusion intervention. The use of TCD in this manner is that of a screening test. A good screening test is one with maximum sensitivity, so that if the test is negative, the condition is not present. In this case, the condition was "clinically evident stroke". The threshold for TCD velocities was set in the STOP trial to detect 97% of all patients with clinically evident stroke. The trial did not measure TCD sensitivity against the presence or progression of intracranial vasculopathy, which is a more proximate cause of stroke in these patients. While nearly all patients with an abnormal TCD by STOP criteria will have vasculopathy, not all patients with vasculopathy will have an abnormal TCD by the STOP TAMV criteria.

It has been further documented that clinically silent strokes in sickle cell patients with normal neurologic and TCD exam are detectable by MR Imaging^[8]. This observation is also concordant with data indicating that patients with silent infarcts on MRI and normal TCD results by the original STOP criteria are more than twice as likely as the unscreened sickle cell population to develop a clinically apparent stroke^[9]. Indeed, even though patients with abnormalities only on MRI frequently have a "normal" neurologic exam, it is becoming more apparent that neuropsychological deficits exist^[10].

In order for TCD screening to maintain its role as an adequate screening test, it must perform close to the level of MRI at least in predicting the presence or progression of intracranial vasculopathy. To this purpose, a number of studies have compared TCD velocity measurements with the presence of

stenosis at MR Angiography. Lowering the TAMV threshold to 165 cm/s could yield a sensitivity of 92% in predicting stenosis on MRI^[11]. Adult studies, however, indicate that the threshold for TAMV would have to be set at 123 cm/s for 100% sensitivity^[12].

The restricted availability of the exam with only a single trained technologist ensured uniformity throughout the study period. The limitations of our study include the small sample size given the relative underutilization of sickle cell services and difficulty of follow-up. While the ultrasound technical exam factors remain well controlled, variations in MRI technique over the 10-year time period could have influenced uniformity of the gold standard. We also did not have the ability to correlate clinical outcomes given the relatively recent transition to an electronic medical record (2010) at our institution. A larger prospective study with the ability to correlate TCD TAMV, PSV, MRI and MRA findings, neuropsychological exam results, and clinically apparent stroke could provide a useful follow-up to the STOP trial to update best practice recommendations for what is one of the leading causes of stroke in pediatric patients.

Based on the data obtained at our institution and using the assumption that the best screening test is the one with the highest sensitivity, the peak systolic velocity could be the measurement of choice for TCD screening. A more specific test with MRI or neuropsychological evaluation should follow in those patients who may have suffered clinically silent ischemic brain injury.

COMMENTS

Background

Without treatment, 11% of children with sickle cell disease will have an ischemic stroke by 20 years of age. Trans Cranial Doppler (TCD) is used as a screening test to prevent this complication in the sickle cell population. A finding of elevated velocities requires further monitoring or transfusion intervention. Velocities can be measured using the time average maximum mean velocity (TAMV) or the peak systolic velocity (PSV) criteria.

Research frontiers

With the growing clinical use of magnetic resonance imaging (MRI)/magnetic resonance angiogram (MRA) to assess sickle cell patients, the sensitivity of TCD should be maximized if it is to maintain its role as a screening test in the sickle cell population.

Innovations and breakthroughs

To the best of our knowledge, there has been no comparison of PSV and TAMV criteria in their ability to predict abnormalities on MRI/MRA.

Applications

Based on the data obtained at our institution and using the assumption that the best screening test is the one with the highest sensitivity, the peak systolic velocity

could be the measurement of choice for TCD screening.

Terminology

The STOP trial is the acronym for Stroke Prevention Trial in Sickle Cell Anemia. It was a significant advance in screening for the complication of ischemic stroke in sickle cell disease as it demonstrated the efficacy of TCD in identifying patients at high risk for ischemic brain injury.

Peer review

It is a very good article.

REFERENCES

- 1 **Ohene-Frempong K**, Weiner SJ, Sleeper LA, Miller ST, Embury S, Moohr JW, Wethers DL, Pegelow CH, Gill FM. Cerebrovascular accidents in sickle cell disease: rates and risk factors. *Blood* 1998; **91**: 288-294 [PMID: 9414296]
- 2 **Pegelow CH**, Adams RJ, McKie V, Abboud M, Berman B, Miller ST, Olivieri N, Vichinsky E, Wang W, Brambilla D. Risk of recurrent stroke in patients with sickle cell disease treated with erythrocyte transfusions. *J Pediatr* 1995; **126**: 896-899 [PMID: 7776091]
- 3 **Adams RJ**, McKie VC, Hsu L, Files B, Vichinsky E, Pegelow C, Abboud M, Gallagher D, Kutlar A, Nichols FT, Bonds DR, Brambilla D. Prevention of a first stroke by transfusions in children with sickle cell anemia and abnormal results on transcranial Doppler ultrasonography. *N Engl J Med* 1998; **339**: 5-11 [PMID: 9647873]
- 4 **Adams R**, McKie V, Nichols F, Carl E, Zhang DL, McKie K, Figueroa R, Litaker M, Thompson W, Hess D. The use of transcranial ultrasonography to predict stroke in sickle cell disease. *N Engl J Med* 1992; **326**: 605-610 [PMID: 1734251]
- 5 **Alexandrov AV**, Brodie DS, McLean A, Hamilton P, Murphy J, Burns PN. Correlation of peak systolic velocity and angiographic measurement of carotid stenosis revisited. *Stroke* 1997; **28**: 339-342 [PMID: 9040686]
- 6 **Jones A**, Granger S, Brambilla D, Gallagher D, Vichinsky E, Woods G, Berman B, Roach S, Nichols F, Adams RJ. Can peak systolic velocities be used for prediction of stroke in sickle cell anemia? *Pediatr Radiol* 2005; **35**: 66-72 [PMID: 15517239]
- 7 **Armstrong-Wells J**, Grimes B, Sidney S, Kronish D, Shiboski SC, Adams RJ, Fullerton HJ. Utilization of TCD screening for primary stroke prevention in children with sickle cell disease. *Neurology* 2009; **72**: 1316-1321 [PMID: 19365052 DOI: 10.1212/WNL.0b013e3181a110da]
- 8 **Siegel MJ**, Luker GD, Glauser TA, DeBaun MR. Cerebral infarction in sickle cell disease: transcranial Doppler US versus neurologic examination. *Radiology* 1995; **197**: 191-194 [PMID: 7568822]
- 9 **Pegelow CH**, Macklin EA, Moser FG, Wang WC, Bello JA, Miller ST, Vichinsky EP, DeBaun MR, Guarini L, Zimmerman RA, Younkin DP, Gallagher DM, Kinney TR. Longitudinal changes in brain magnetic resonance imaging findings in children with sickle cell disease. *Blood* 2002; **99**: 3014-3018 [PMID: 11929794]
- 10 **Platt OS**. Prevention and management of stroke in sickle cell anemia. *Hematology Am Soc Hematol Educ Program* 2006; **Abstract**: 54-57 [PMID: 17124040]
- 11 **Arkuszewski M**, Krejza J, Chen R, Kwiatkowski JL, Ichord R, Zimmerman R, Ohene-Frempong K, Melhem ER. Sickle cell disease in children: accuracy of imaging transcranial Doppler ultrasonography in detection of intracranial arterial stenosis. *Neuroradiol J* 2012; **25**: 402-410 [PMID: 24029032]
- 12 **Silva GS**, Vicari P, Figueiredo MS, Carrete H, Idagawa MH, Massaro AR. Brain magnetic resonance imaging abnormalities in adult patients with sickle cell disease: correlation with transcranial Doppler findings. *Stroke* 2009; **40**: 2408-2412 [PMID: 19443807]

P- Reviewer: Al-Haggag M S- Editor: Ji FF L- Editor: A
E- Editor: Wu HL





Published by **Baishideng Publishing Group Inc**

8226 Regency Drive, Pleasanton, CA 94588, USA

Telephone: +1-925-223-8242

Fax: +1-925-223-8243

E-mail: bpgoffice@wjgnet.com

Help Desk: <http://www.wjgnet.com/esps/helpdesk.aspx>

<http://www.wjgnet.com>

